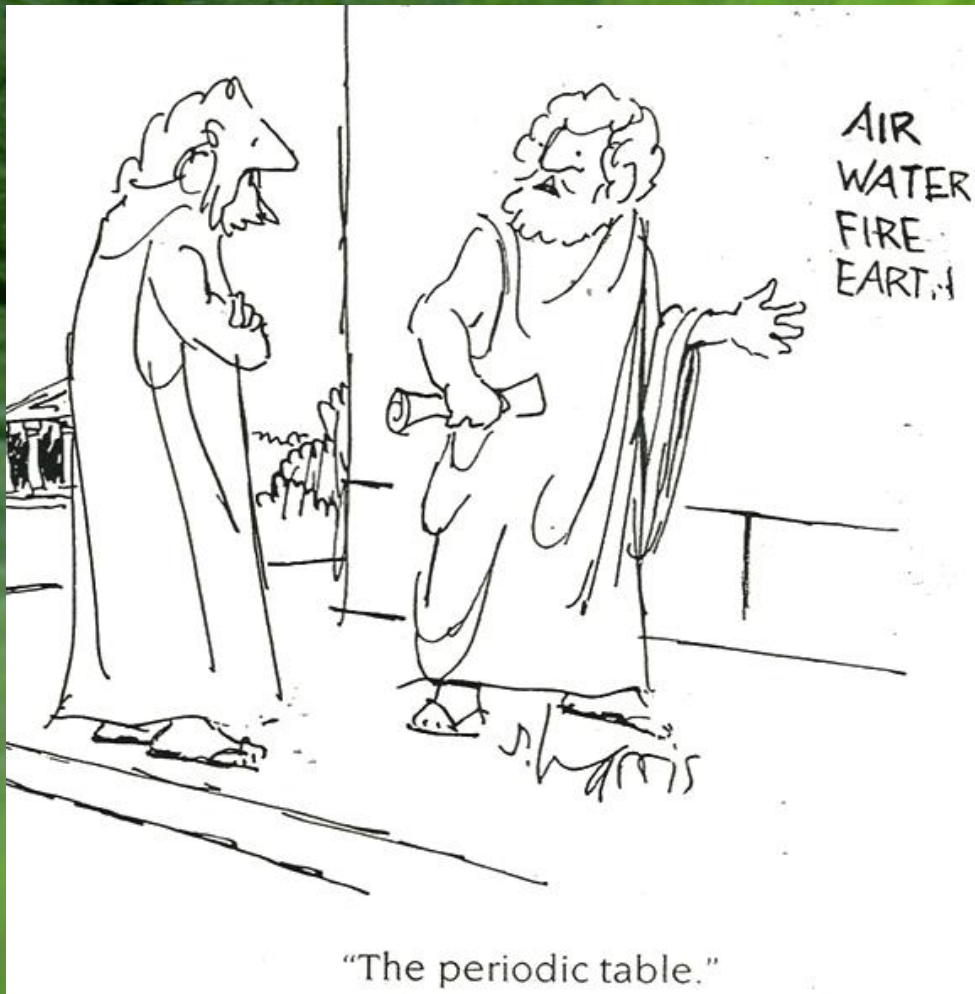


Tight-Binding Approximation



Faculty of Physics UW
Jacek.Szczytko@fuw.edu.pl



The band theory of solids.

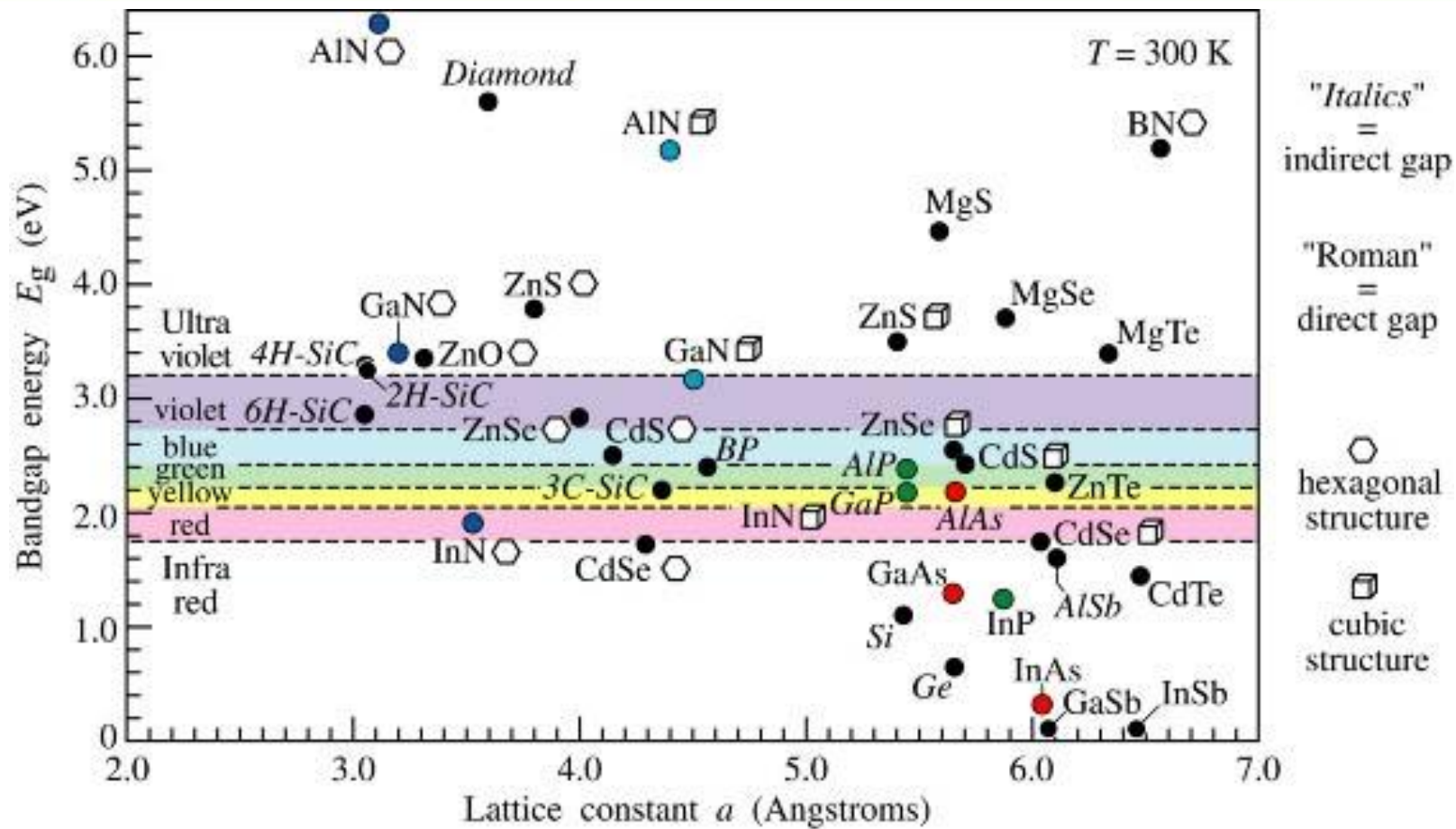


Fig. 11.4. Room-temperature bandgap energy versus lattice constant of common elemental and binary compound semiconductors.

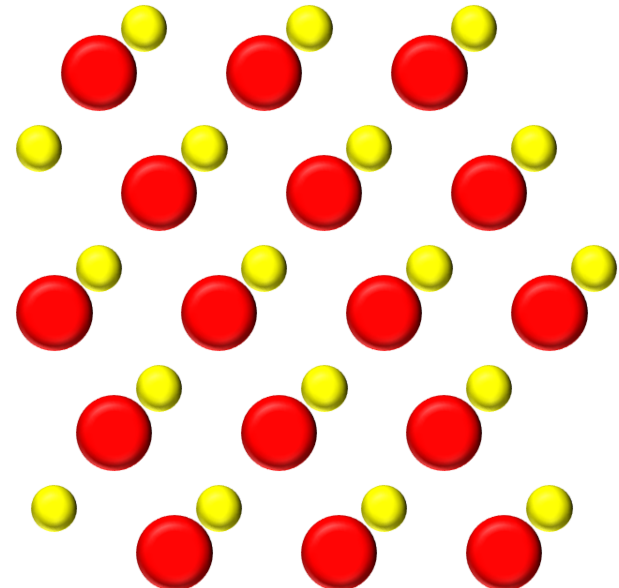
Periodic potential

Bloch theorem

$$\varphi_{n,\vec{k}}(\vec{r}) = u_{n,\vec{k}}(\vec{r}) e^{i\vec{k}\vec{r}}$$

Bloch wave,
Bloch function

Bloch amplitude,
Bloch envelope



The solution of the one-electron Schrödinger equation for a periodic potential has a form of modulated plane wave:

$$u_{n,\vec{k}}(\vec{r}) = u_{n,\vec{k}}(\vec{r} + \vec{R})$$

We introduced coefficient n for different solutions corresponding to the same \vec{k} (*index*). \vec{k} -vector is an element of the *first Brillouin zone*.

$$u_{n,\vec{k}}(\vec{r}) = \sum_{\vec{G}} C_{\vec{k}-\vec{G}} e^{i\vec{G}\vec{r}}$$

Periodic potential

Bloch theorem

Proof:

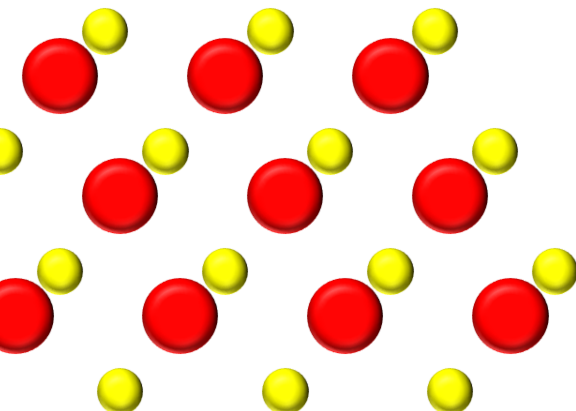
Translation operator $\hat{T}_{\vec{R}}$ $\hat{T}_{\vec{R}}(f(\vec{r})) = f(\vec{r} + \vec{R})$

Periodic potential of the crystal lattice: $\hat{T}_{\vec{R}}(V(\vec{r})) = V(\vec{r} + \vec{R})$

Hamiltonian with periodic potential

$$\hat{T}_{\vec{R}}(\hat{H}(\vec{r})\psi(\vec{r})) = \hat{H}(\vec{r} + \vec{R})\psi(\vec{r} + \vec{R}) = \hat{H}(\vec{r})\psi(\vec{r} + \vec{R}) = \hat{H}(\vec{r})\hat{T}_{\vec{R}}(\psi(\vec{r}))$$

$$\hat{T}_{\vec{R}}\hat{T}_{\vec{R}'}\psi(\vec{r}) = \psi(\vec{r} + \vec{R} + \vec{R}') = \hat{T}_{\vec{R}'}\hat{T}_{\vec{R}}\psi(\vec{r})$$



operators are commutative!

Eigenfunctions $\psi_{n,\vec{k}}(\vec{r})$ of the translation operator $\hat{T}_{\vec{R}}$:

$$\hat{T}_{\vec{R}}\psi_{n,\vec{k}}(\vec{r}) = C(\vec{R})\psi_{n,\vec{k}}(\vec{r}) = e^{if(\vec{R})}\psi_{n,\vec{k}}(\vec{r}) \quad |C(\vec{R})|^2 = 1$$

$$\text{where } f(\vec{R} + \vec{R}') = f(\vec{R}) + f(\vec{R}')$$

$$f(0) = 0$$

$$\Rightarrow f(\vec{R}) = \vec{k}\vec{R}$$

Periodic potential

Bloch theorem

Proof:

Translation operator $\hat{T}_{\vec{R}}$ $\hat{T}_{\vec{R}}(f(\vec{r})) = f(\vec{r} + \vec{R})$

Eigenfunctions $\psi_{n,\vec{k}}(\vec{r})$ of the operator $\hat{T}_{\vec{R}}$

$$\hat{T}_{\vec{R}}\psi(\vec{r}) = C(\vec{R})\psi_{n,\vec{k}}(\vec{r}) = e^{i\vec{k}\vec{R}}\psi_{n,\vec{k}}(\vec{r})$$

We denote our eigenfunction $\psi_{n,\vec{k}}(\vec{r})$ where n distinguishes the different functions of the same \vec{k} . Let us define:

$$u_{n,\vec{k}} = \psi_{n,\vec{k}}(\vec{r})e^{-i\vec{k}\vec{r}}$$

periodic function

$$\hat{T}_{\vec{R}}(u_{n,\vec{k}}) = \hat{T}_{\vec{R}}\left(\psi_{n,\vec{k}}(\vec{r})e^{-i\vec{k}\vec{r}}\right) = e^{i\vec{k}\vec{R}}\psi_{n,\vec{k}}(\vec{r})e^{-i\vec{k}(\vec{r}+\vec{R})} = \psi_{n,\vec{k}}(\vec{r})e^{-i\vec{k}\vec{r}} = u_{n,\vec{k}}$$

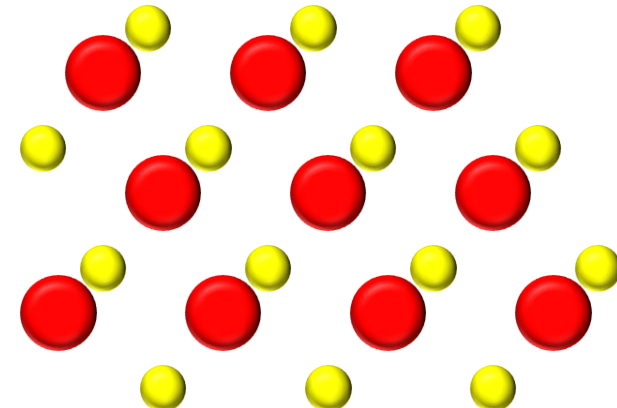
Thus:

$$\boxed{\psi_{n,\vec{k}}(\vec{r}) = u_{n,\vec{k}}e^{i\vec{k}\vec{r}}}$$

The eigenstates of the electron in a periodic potential are characterized by two quantum numbers \vec{k} and n

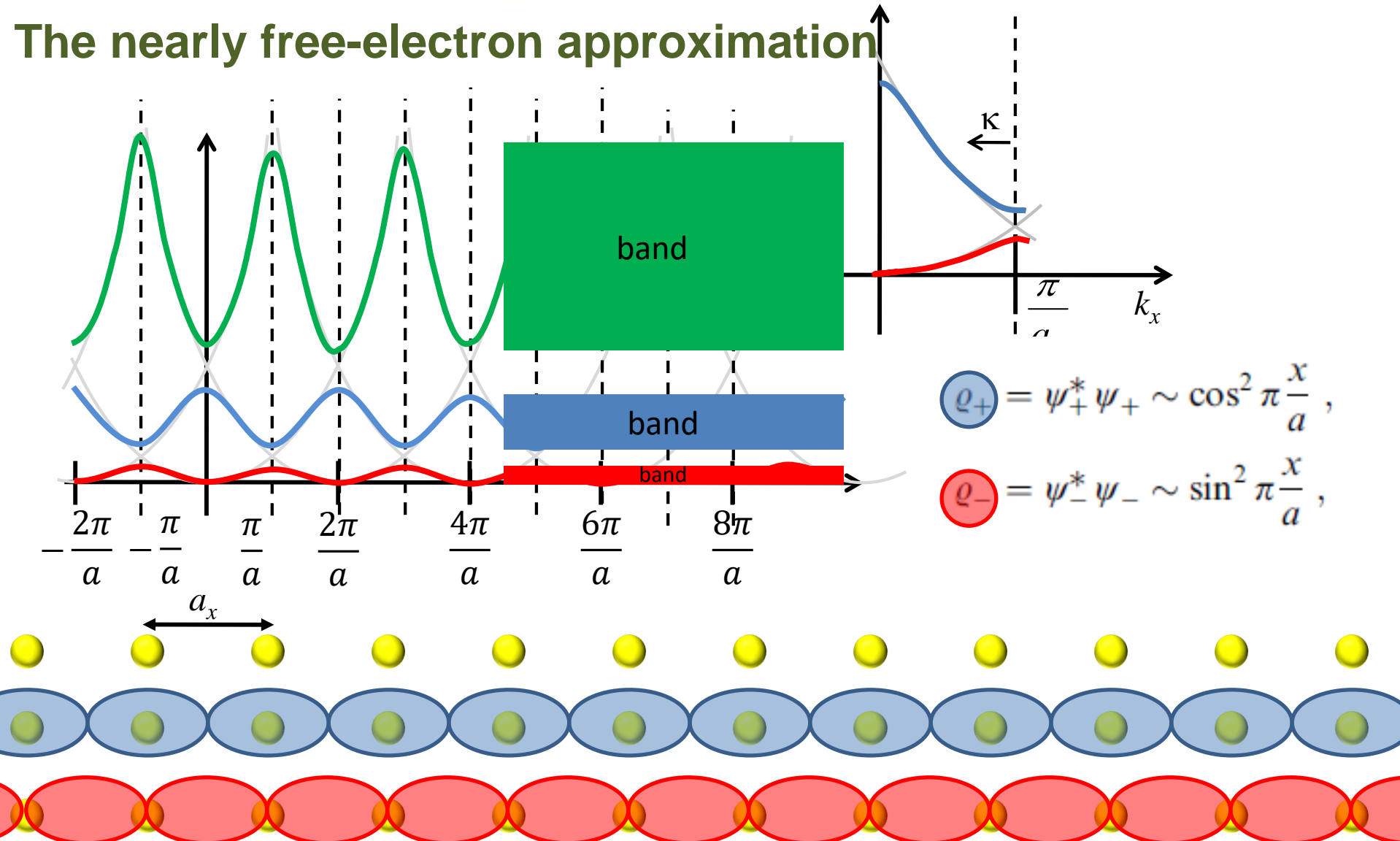
\vec{k} – wave vector

n – describes the energy bands (for a moment!)



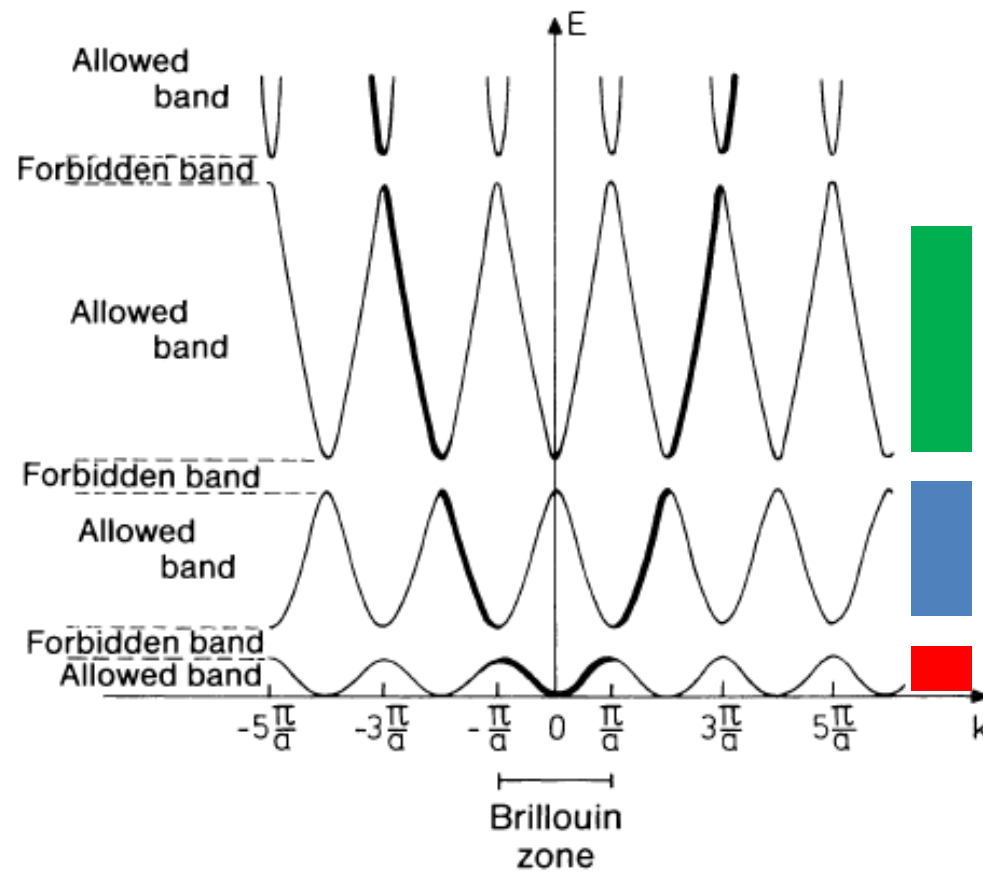
Periodic potential

The nearly free-electron approximation



The electronic band structure

- It is convenient to present the energies only in the 1st Brillouin zone.
- The electron state in the solid state is given by the wave vector of the 1st Brillouin zone, band number and a spin.



The electronic band structure

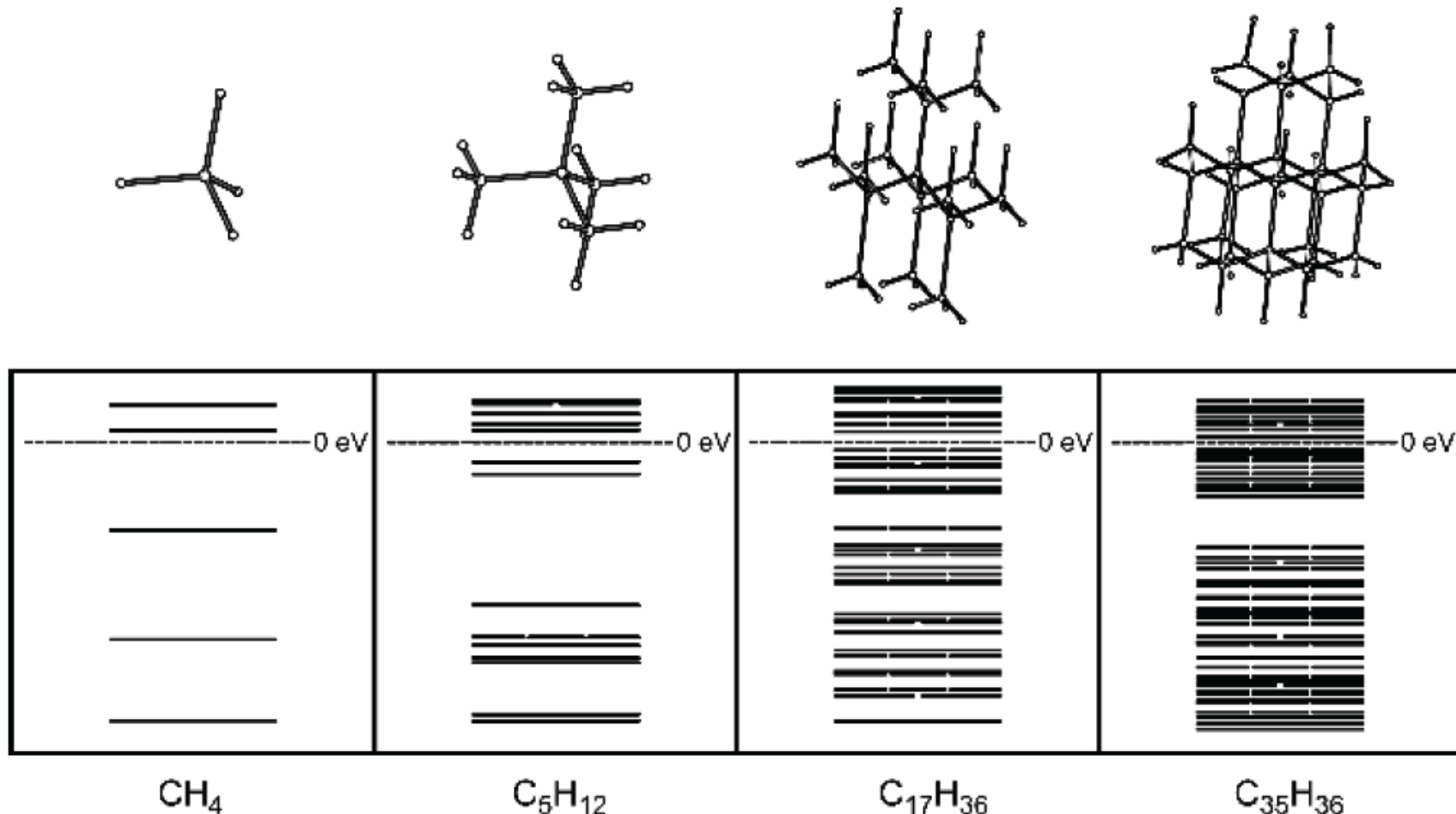


Fig. 2.3 Development of the diamond band gap

The electronic band structure

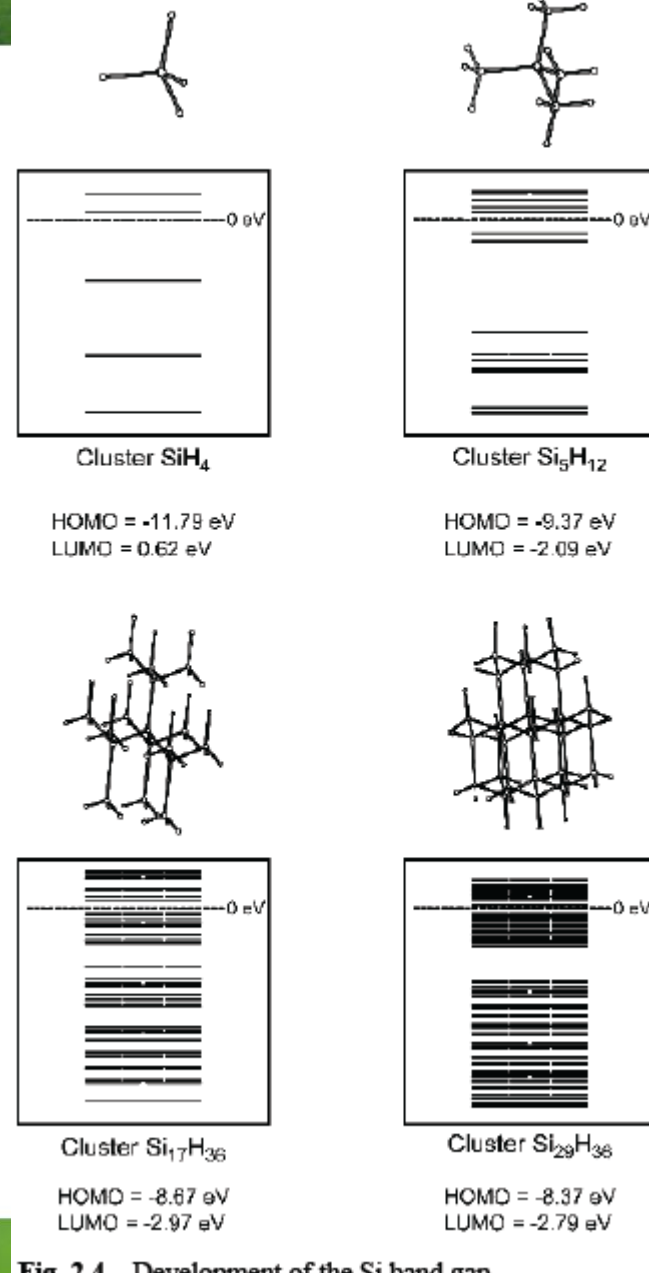


Fig. 2.4 Development of the Si band gap

Tight-Binding Approximation

We describe the crystal electrons in terms of a linear superposition of atomic eigenfunctions (LCAO – Linear Combination of Atomic Orbitals) $H = H_A + V'$:

$$H_A(\vec{r} - \vec{R}_n)\varphi_j(\vec{r} - \vec{R}_n) = E_j\varphi_j(\vec{r} - \vec{R}_n)$$

Equation for the free atoms that form the crystal

$$H_A = -\frac{\hbar^2}{2m}\Delta + V_A(\vec{r} - \vec{R}_n)$$

j -th state e

Atom in position \vec{R}_n

$$H = H_A + V' = -\frac{\hbar^2}{2m}\Delta + V_A(\vec{r} - \vec{R}_n) + \sum_{m \neq n} V_A(\vec{r} - \vec{R}_m)$$

Perturbation: the influence of atoms in the neighborhood of \vec{R}_m :

$$V'(\vec{r} - \vec{R}_n) = \sum_{m \neq n} V_A(\vec{r} - \vec{R}_m)$$

Good for valence band of covalent crystals, d -orbital bands etc.

Tight-Binding Approximation

Approximate solution in the form of the Bloch function:

$$\Phi_{j,\vec{k}}(\vec{r}) = \sum_n a_n \varphi_j(\vec{r} - \vec{R}_n) = \sum_n \exp(i \vec{k} \vec{R}_n) \varphi_j(\vec{r} - \vec{R}_n)$$

Check:

blackboard

$$\begin{aligned}\Phi_{j,\vec{k}+\vec{G}}(\vec{r}) &= \Phi_{j,\vec{k}}(\vec{r}) \\ \Phi_{j,\vec{k}}(\vec{r} + \vec{T}) &= \exp(i \vec{k} \vec{T}) \Phi_{j,\vec{k}}(\vec{r})\end{aligned}$$

Energies determined by the variational method:

$$E(\vec{k}) \leq \frac{\langle \Phi_{j,\vec{k}}(\vec{r}) | H | \Phi_{j,\vec{k}}(\vec{r}) \rangle}{\langle \Phi_{j,\vec{k}}(\vec{r}) | \Phi_{j,\vec{k}}(\vec{r}) \rangle}$$

Expression

$$\langle \Phi_{j,\vec{k}}(\vec{r}) | \Phi_{j,\vec{k}}(\vec{r}) \rangle = \sum_{n,m} \exp[i \vec{k}(\vec{R}_n - \vec{R}_m)] \int \varphi_j^*(\vec{r} - \vec{R}_m) \varphi_j(\vec{r} - \vec{R}_n) dV$$

can be easily simplify assuming a small overlap of wave functions for $n \neq m$

$$\langle \Phi_{j,\vec{k}}(\vec{r}) | \Phi_{j,\vec{k}}(\vec{r}) \rangle = \sum_n \int \varphi_j^*(\vec{r} - \vec{R}_n) \varphi_j(\vec{r} - \vec{R}_n) dV = \dots$$

How many?

Tight-Binding Approximation

Approximate solution in the form of the Bloch function:

$$\Phi_{j,\vec{k}}(\vec{r}) = \sum_n a_n \varphi_j(\vec{r} - \vec{R}_n) = \sum_n \exp(i \vec{k} \vec{R}_n) \varphi_j(\vec{r} - \vec{R}_n)$$

Check:

$$\begin{aligned}\Phi_{j,\vec{k}+\vec{G}}(\vec{r}) &= \Phi_{j,\vec{k}}(\vec{r}) \\ \Phi_{j,\vec{k}}(\vec{r} + \vec{T}) &= \exp(i \vec{k} \vec{T}) \Phi_{j,\vec{k}}(\vec{r})\end{aligned}$$

Energies determined by the variational method:

$$E(\vec{k}) \leq \frac{\langle \Phi_{j,\vec{k}}(\vec{r}) | H | \Phi_{j,\vec{k}}(\vec{r}) \rangle}{\langle \Phi_{j,\vec{k}}(\vec{r}) | \Phi_{j,\vec{k}}(\vec{r}) \rangle}$$

$$\begin{aligned}E(\vec{k}) &\approx \frac{1}{N} \langle \Phi_{j,\vec{k}}(\vec{r}) | H | \Phi_{j,\vec{k}}(\vec{r}) \rangle = \\ &= \sum_{n,m} \exp[i \vec{k}(\vec{R}_n - \vec{R}_m)] \int \varphi_j^*(\vec{r} - \vec{R}_m) [E_j + V'(\vec{r} - \vec{R}_n)] \varphi_j(\vec{r} - \vec{R}_n) dV\end{aligned}$$

Tight-Binding Approximation

Approximate solution in the form of the Bloch function:

$$\Phi_{j,\vec{k}}(\vec{r}) = \sum_n a_n \varphi_j(\vec{r} - \vec{R}_n) = \sum_n \exp(i \vec{k} \vec{R}_n) \varphi_j(\vec{r} - \vec{R}_n)$$

Check:

$$\begin{aligned}\Phi_{j,\vec{k}+\vec{G}}(\vec{r}) &= \Phi_{j,\vec{k}}(\vec{r}) \\ \Phi_{j,\vec{k}}(\vec{r} + \vec{T}) &= \exp(i \vec{k} \vec{T}) \Phi_{j,\vec{k}}(\vec{r})\end{aligned}$$

Energies determined by the variational method:

$$E(\vec{k}) \leq \frac{\langle \Phi_{j,\vec{k}}(\vec{r}) | H | \Phi_{j,\vec{k}}(\vec{r}) \rangle}{\langle \Phi_{j,\vec{k}}(\vec{r}) | \Phi_{j,\vec{k}}(\vec{r}) \rangle}$$

$$\begin{aligned}E(\vec{k}) &\approx \frac{1}{N} \langle \Phi_{j,\vec{k}}(\vec{r}) | H | \Phi_{j,\vec{k}}(\vec{r}) \rangle = \\ &= \sum_{n,m} \exp[i \vec{k}(\vec{R}_n - \vec{R}_m)] \int \varphi_j^*(\vec{r} - \vec{R}_m) [E_j + V'(\vec{r} - \vec{R}_n)] \varphi_j(\vec{r} - \vec{R}_n) dV\end{aligned}$$

Only diagonal terms $\vec{R}_n = \vec{R}_m$ in E_j

Only the vicinity of \vec{R}_n

Tight-Binding Approximation

$$E(\vec{k}) \approx \frac{1}{N} \left\langle \Phi_{j,\vec{k}}(\vec{r}) \middle| H \middle| \Phi_{j,\vec{k}}(\vec{r}) \right\rangle = \\ = \sum_{n,m} \exp[i\vec{k}(\vec{R}_n - \vec{R}_m)] \int \varphi_j^*(\vec{r} - \vec{R}_m) [E_j + V'(\vec{r} - \vec{R}_n)] \varphi_j(\vec{r} - \vec{R}_n) dV$$

Only diagonal terms $\vec{R}_n = \vec{R}_m$ in E_j

Only the vicinity of \vec{R}_n

When the atomic states $\varphi_j(\vec{r} - \vec{R}_n)$ are spherically symmetric (*s*-states), then overlap integrals depend only on the distance between atoms:

$$E_n(\vec{k}) \approx E_j - A_j - B_j \sum_m \exp[i\vec{k}(\vec{R}_n - \vec{R}_m)]$$

$$A_j = - \int \varphi_j^*(\vec{r} - \vec{R}_n) [V'(\vec{r} - \vec{R}_n)] \varphi_j(\vec{r} - \vec{R}_n) dV$$

$$B_j = - \int \varphi_j^*(\vec{r} - \vec{R}_m) [V'(\vec{r} - \vec{R}_n)] \varphi_j(\vec{r} - \vec{R}_n) dV$$

Restricted to only the nearest neighbours of \vec{R}_n

Tight-Binding Approximation

When the atomic states $\varphi_j(\vec{r} - \vec{R}_n)$ are spherically symmetric (*s*-states), then overlap integrals depend only on the distance between atoms:

$$E_n(\vec{k}) \approx E_j - A_j - B_j \sum_m \exp[i\vec{k}(\vec{R}_n - \vec{R}_m)]$$

$$A_j = - \int \varphi_j^*(\vec{r} - \vec{R}_n) [V'(\vec{r} - \vec{R}_n)] \varphi_j(\vec{r} - \vec{R}_n) dV$$

$$B_j = - \int \varphi_j^*(\vec{r} - \vec{R}_m) [V'(\vec{r} - \vec{R}_n)] \varphi_j(\vec{r} - \vec{R}_n) dV$$

The result of the summation depends on the symmetry of the lattice:

For *sc* structure: $\vec{R}_n - \vec{R}_m = (\pm a, 0, 0); (0, \pm a, 0); (0, 0, \pm a)$;

$$E_n(\vec{k}) \approx E_j - A_j - 2B_j [\cos k_x a + \cos k_y a + \cos k_z a]$$

For *bcc* structure :

$$E_n(\vec{k}) \approx E_j - A_j - 8B_j \cos\left(\frac{k_x a}{2}\right) \cos\left(\frac{k_y a}{2}\right) \cos\left(\frac{k_z a}{2}\right)$$

For *fcc* structure :

$$E_n(\vec{k}) \approx E_j - A_j - 4B_j \left[\cos\left(\frac{k_x a}{2}\right) \cos\left(\frac{k_y a}{2}\right) + c.p. \right]$$

Tight-Binding Approximation

For sc structure: $\vec{R}_n - \vec{R}_m = (\pm a, 0, 0); (0, \pm a, 0); (0, 0, \pm a)$;

$$E_n(\vec{k}) \approx E_j - A_j - 2B_j[\cos k_x a + \cos k_y a + \cos k_z a]$$

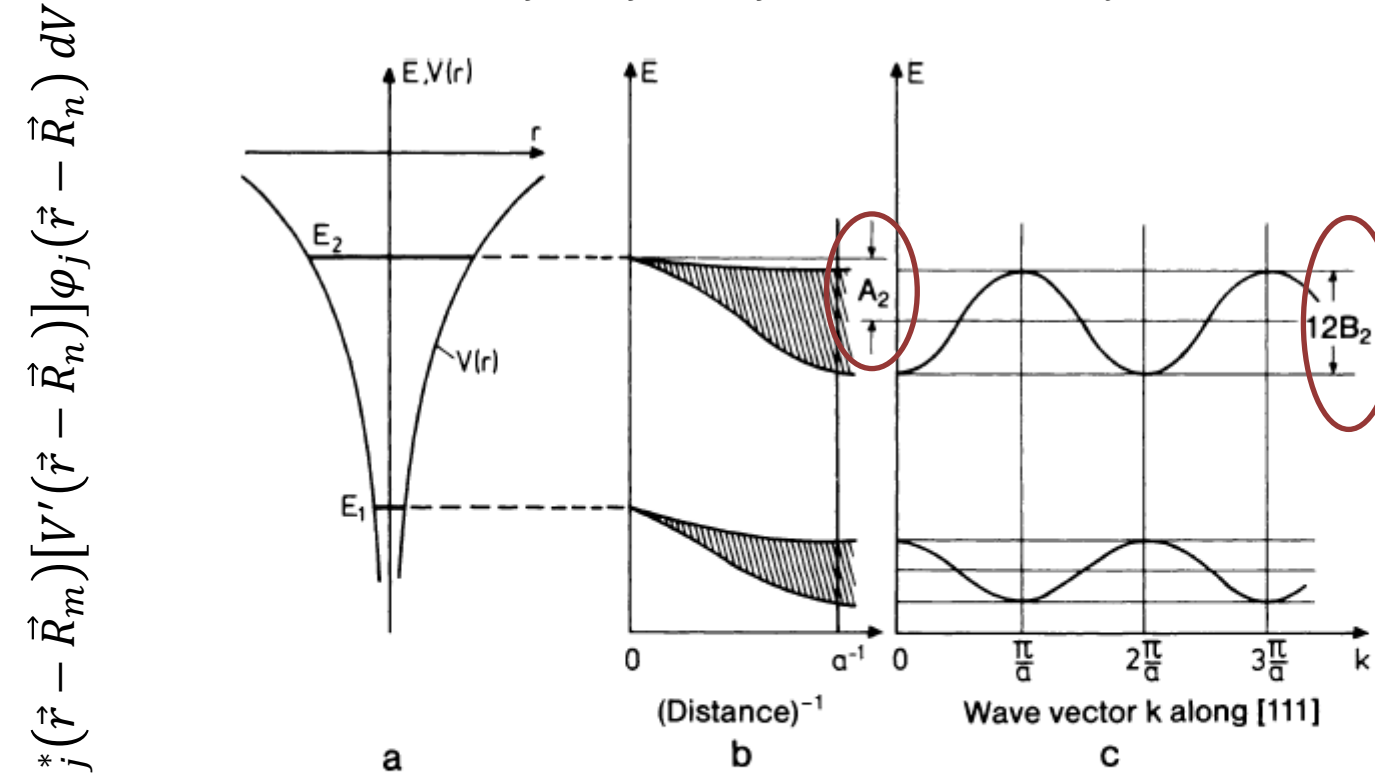


Fig. 7.8 a–c. Qualitative illustration of the result of a tight-binding calculation for a primitive cubic lattice with lattice constant a . (a) Position of the energy levels E_1 and E_2 in the potential $V(r)$ of the free atom. (b) Reduction and broadening of the levels E_1 and E_2 as a function of the reciprocal atomic separation r^{-1} . At the equilibrium separation a the mean energy decrease is A and the width of the band is $12B$. (c) Dependence of the one-electron energy E on the wave vector $k(1, 1, 1)$ in the direction of the main diagonal [111].

$$B_j = - \int \varphi_j^*(\vec{r} - \vec{R}_m) [V'(\vec{r} - \vec{R}_n)] \varphi_j(\vec{r} - \vec{R}_n) dV$$

Tight-Binding Approximation

For sc structure: $\vec{R}_n - \vec{R}_m = (\pm a, 0, 0); (0, \pm a, 0); (0, 0, \pm a)$;

$$E_n(\vec{k}) \approx E_j - A_j - 2B_j[\cos k_x a + \cos k_y a + \cos k_z a]$$

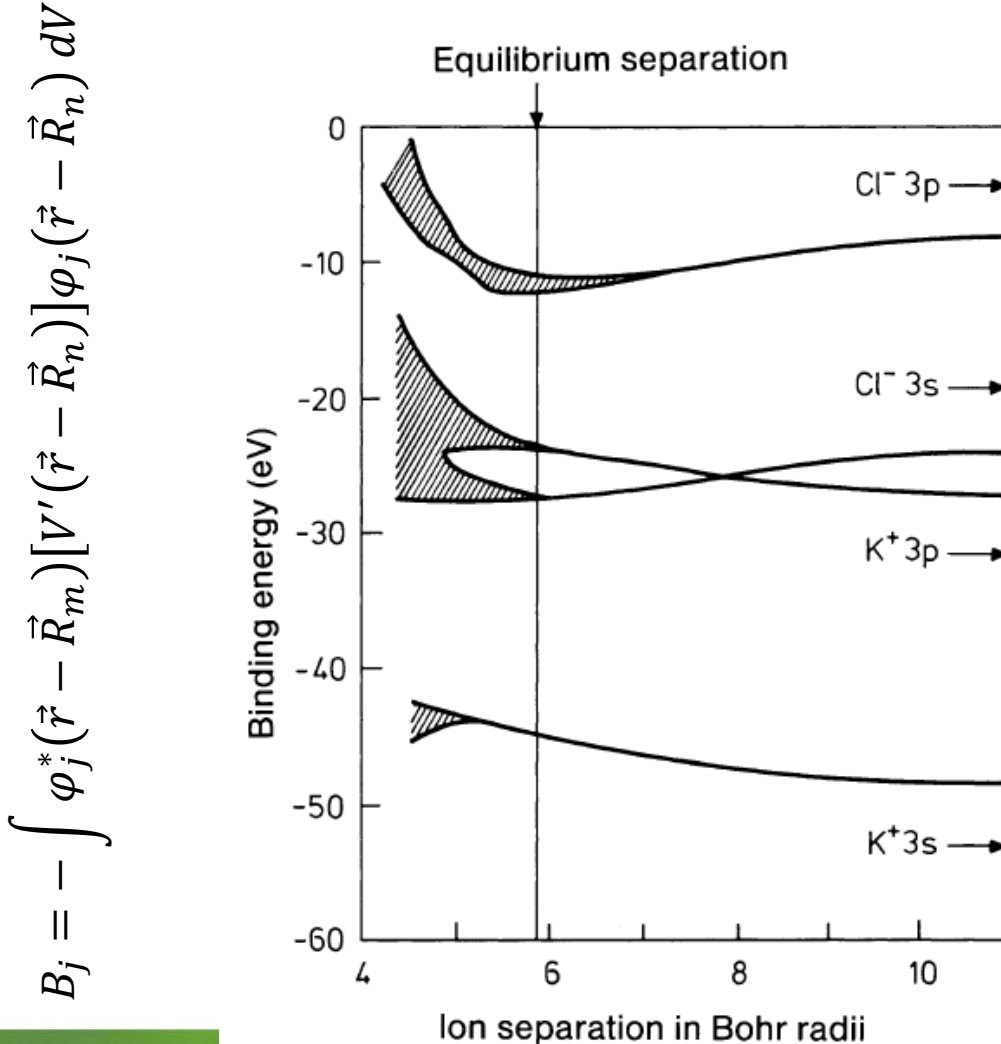
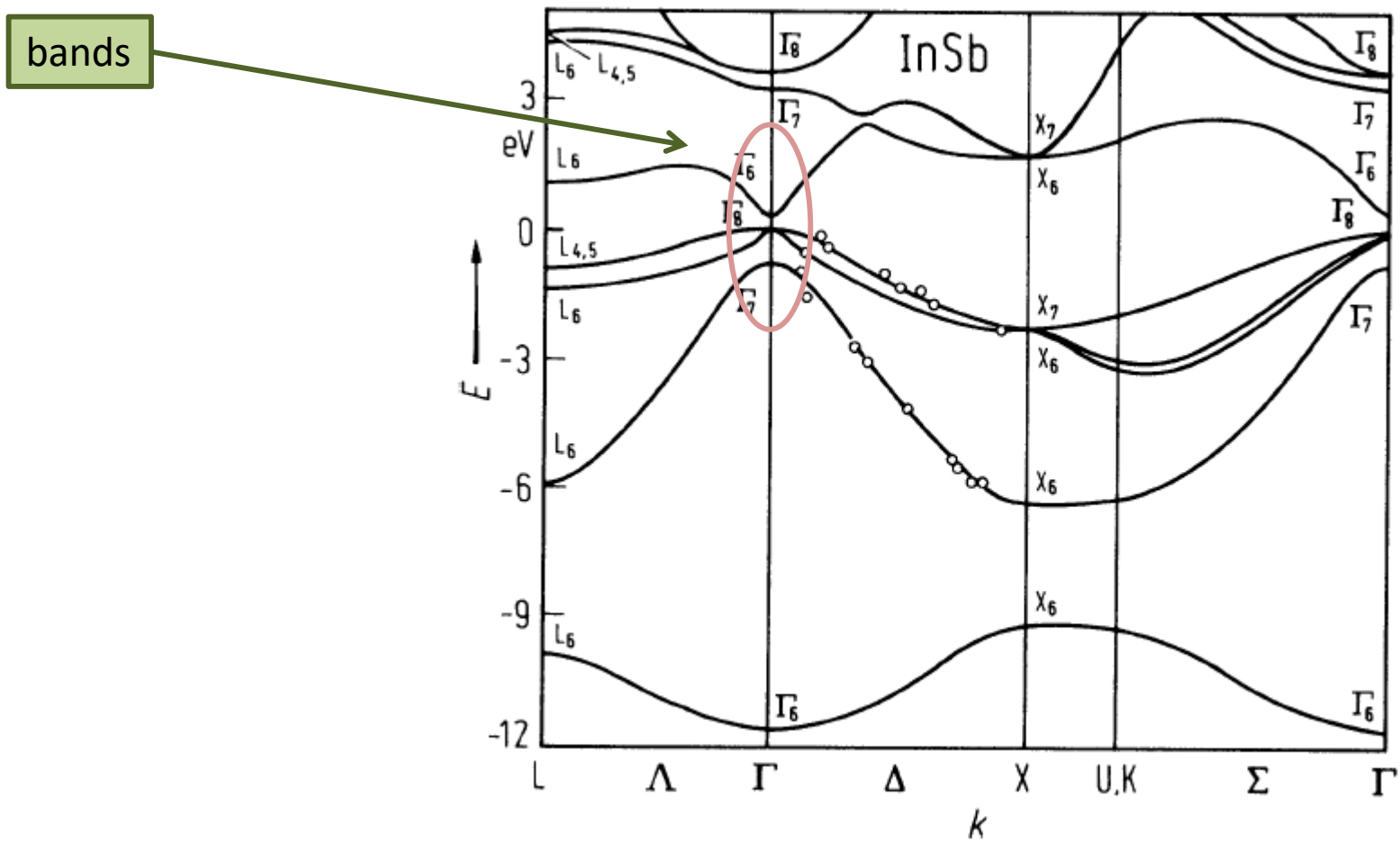


Fig. 7.10. The four highest occupied energy bands of KCl calculated as a function of the ionic separation in Bohr radii ($a_0 = 5.29 \times 10^{-9}$ cm). The energy levels in the free ions are indicated by arrows. (After [7.2])

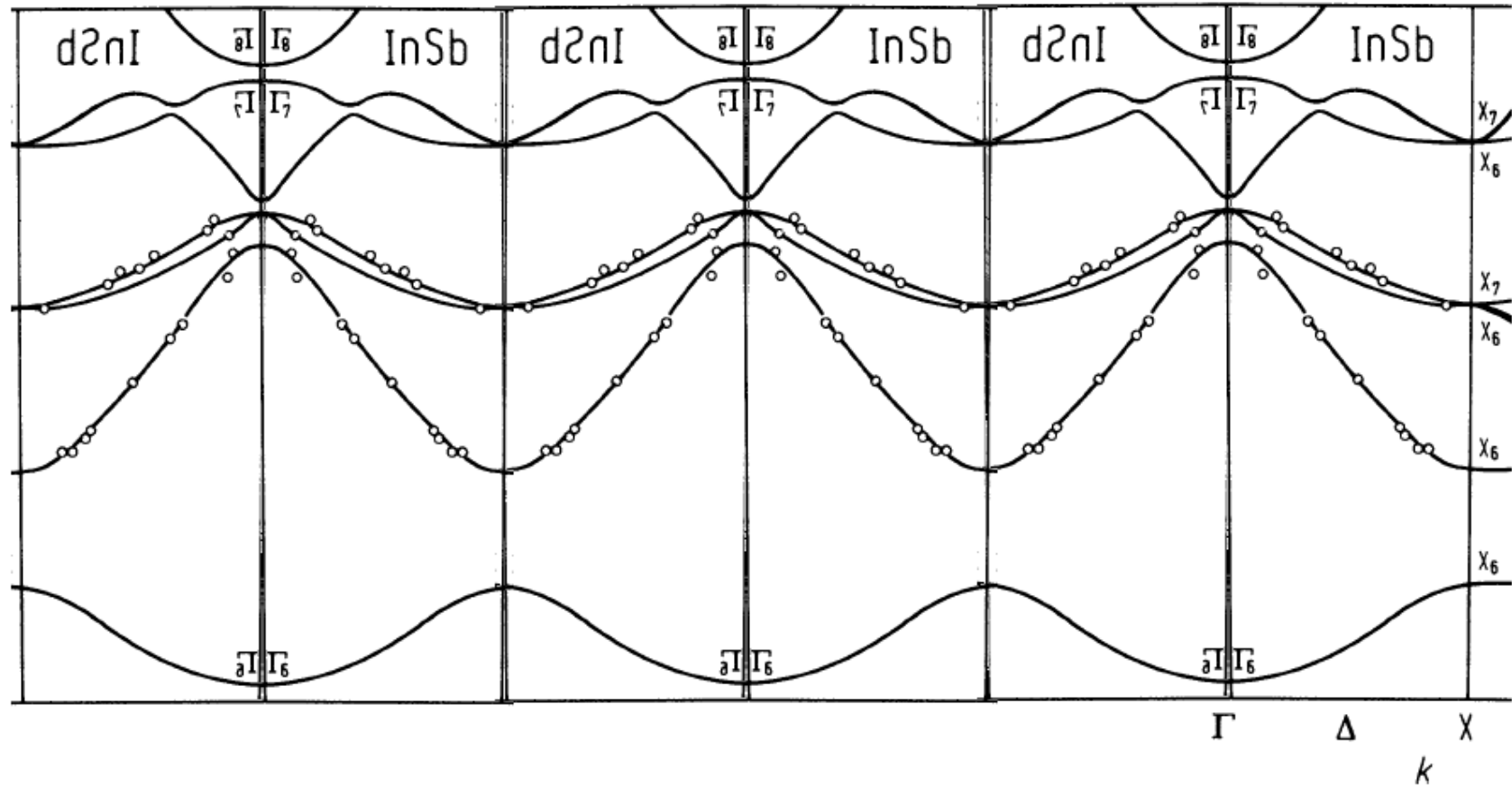
The electronic band structure



Expanding $E_n(\vec{k}) = \left(E_n - \frac{\hbar^2 \vec{k}^2}{2m} \right)$ near extremum, e.g. $k = 0$:

Landolt-Boernstein

The electronic band structure



Expanding $E_n(\vec{k}) = \left(E_n - \frac{\hbar^2 \vec{k}^2}{2m} \right)$ near extremum, e.g. $k = 0$:

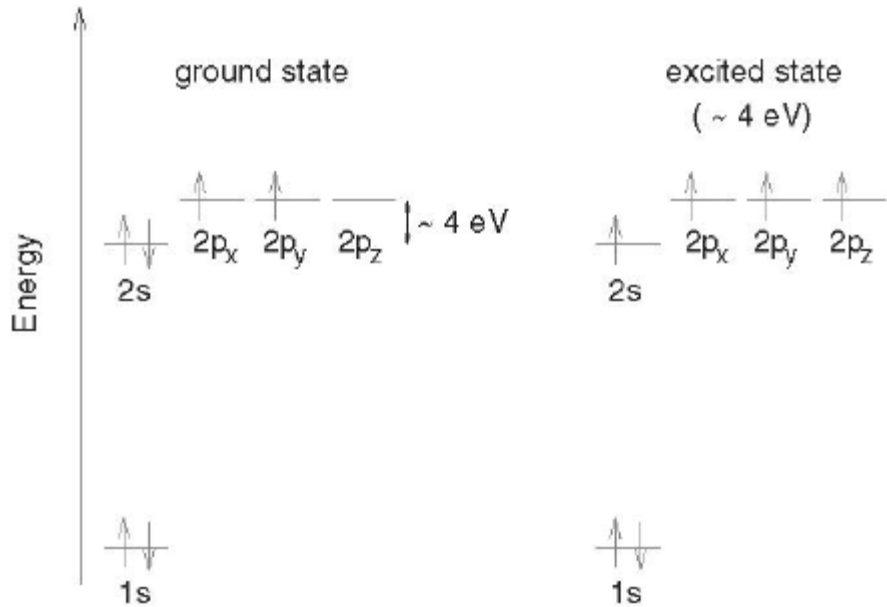
Landolt-Boernstein

Tight-Binding Approximation

Linear dispersion relation in graphene:

Tight binding approach with the only nearest neighbors interaction [P. R. Wallace, „The Band Theory of Graphite”, Physical Review 71, 622 (1947).] gives:

$$E(\vec{k}) = \pm \sqrt{\gamma_0^2 \left(1 + 4 \cos^2 \frac{k_y a}{2} + 4 \cos \frac{k_y a}{2} \cdot \cos \frac{k_x \sqrt{3} a}{2} \right)} \approx \hbar \tilde{c} |\vec{k} - \vec{k}_i|$$



$$|\phi_1\rangle = \frac{1}{\sqrt{3}} |2s\rangle + \sqrt{\frac{2}{3}} |2p_x\rangle$$

$$|\phi_2\rangle = \frac{1}{\sqrt{3}} |2s\rangle - \frac{1}{\sqrt{6}} |2p_x\rangle + \frac{1}{\sqrt{2}} |2p_y\rangle$$

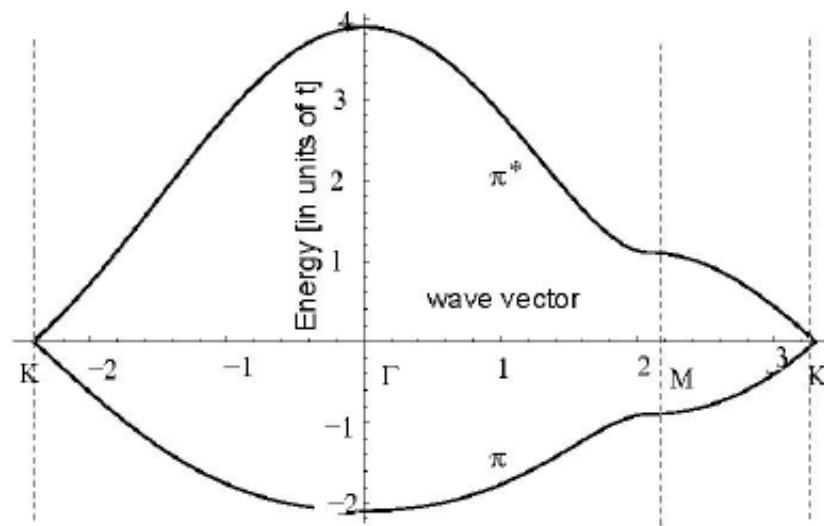
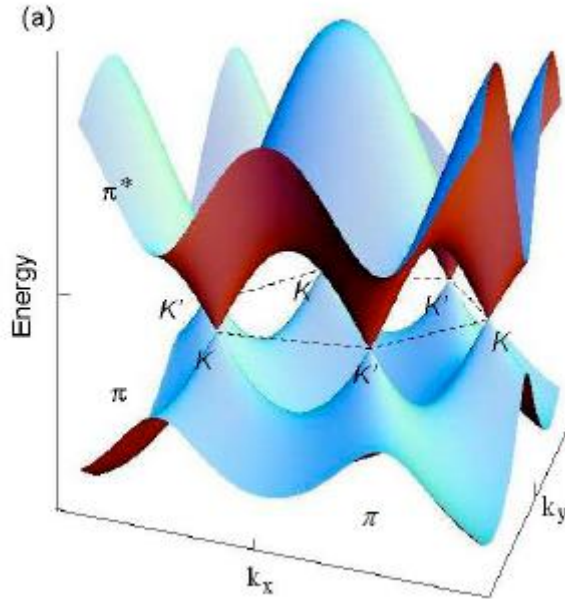
$$|\phi_3\rangle = \frac{1}{\sqrt{3}} |2s\rangle - \frac{1}{\sqrt{6}} |2p_x\rangle - \frac{1}{\sqrt{2}} |2p_y\rangle$$

Tight-Binding Approximation

Linear dispersion relation in graphene:

Tight binding approach with the only nearest neighbors interaction [P. R. Wallace, „The Band Theory of Graphite”, Physical Review 71, 622 (1947).] gives:

$$E(\vec{k}) = \pm \sqrt{\gamma_0^2 \left(1 + 4 \cos^2 \frac{k_y a}{2} + 4 \cos \frac{k_y a}{2} \cdot \cos \frac{k_x \sqrt{3} a}{2} \right)} \approx \hbar \tilde{c} |\vec{k} - \vec{k}_i|$$

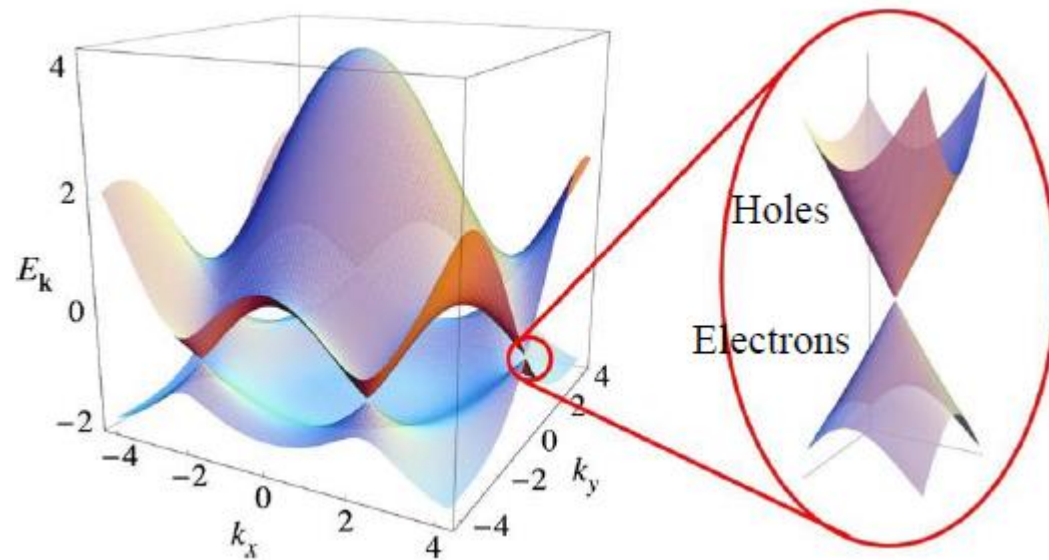


Tight-Binding Approximation

Linear dispersion relation in graphene:

Tight binding approach with the only nearest neighbors interaction [P. R. Wallace, „The Band Theory of Graphite”, Physical Review 71, 622 (1947).] gives:

$$E(\vec{k}) = \pm \sqrt{\gamma_0^2 \left(1 + 4 \cos^2 \frac{k_y a}{2} + 4 \cos \frac{k_y a}{2} \cdot \cos \frac{k_x \sqrt{3} a}{2} \right)} \approx \hbar \tilde{c} |\vec{k} - \vec{k}_i|$$



Tight-Binding Approximation

Linear dispersion relation in graphene:

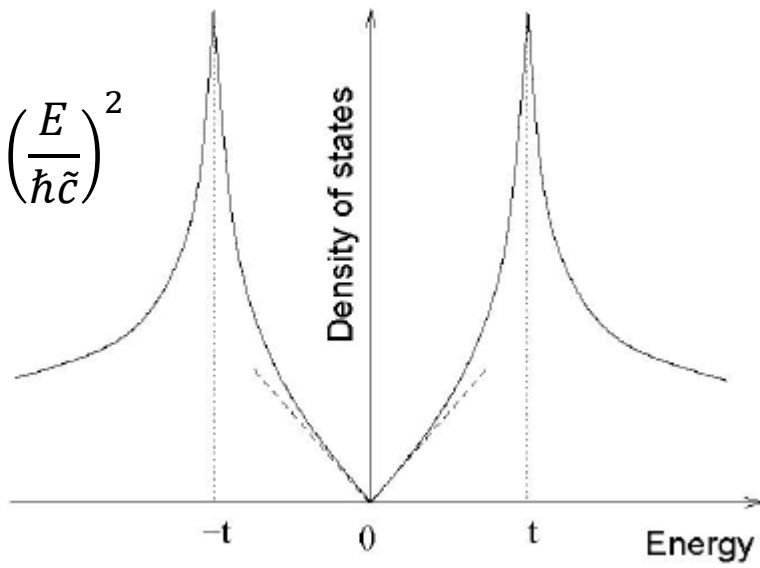
Tight binding approach with the only nearest neighbors interaction [P. R. Wallace, „The Band Theory of Graphite”, Physical Review 71, 622 (1947).] gives:

$$E(\vec{k}) = \pm \sqrt{\gamma_0^2 \left(1 + 4 \cos^2 \frac{k_y a}{2} + 4 \cos \frac{k_y a}{2} \cdot \cos \frac{k_x \sqrt{3} a}{2} \right)} \approx \hbar \tilde{c} |\vec{k} - \vec{k}_i|$$

The number of states in the volume of πk^2 :

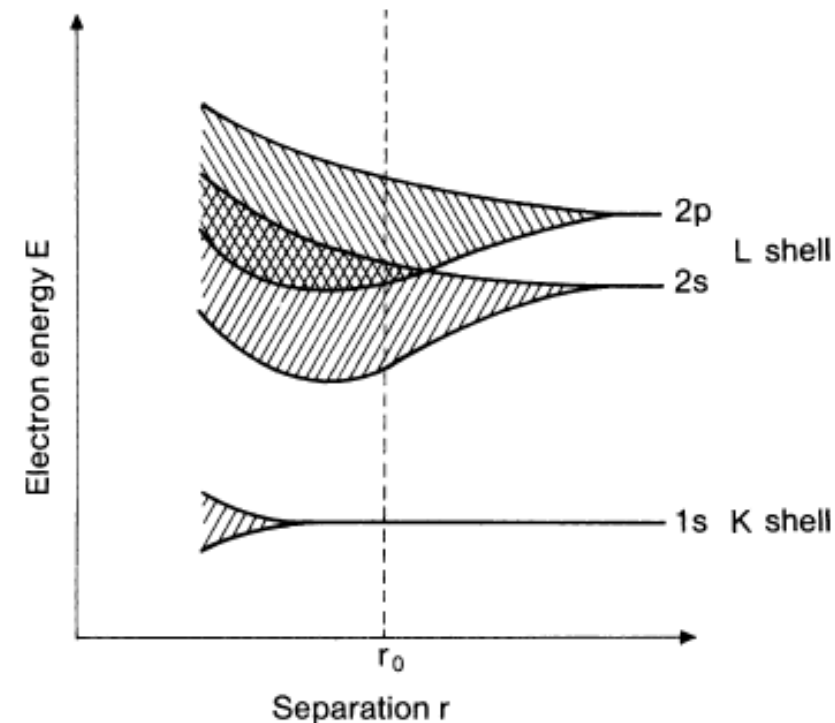
$$N(E) = \frac{2}{(2\pi)^2} \pi k^2 = \frac{2}{(2\pi)^2} \pi (\vec{k} - \vec{k}_i)^2 = \frac{2}{(2\pi)^2} \pi \left(\frac{E}{\hbar \tilde{c}} \right)^2$$

$$\rho(E) = \frac{\partial N(E)}{\partial E} = \frac{E}{\pi (\hbar \tilde{c})^2}$$



Tight-Binding Approximation

The existence of the band structure arising from the discrete energy levels of isolated atoms due to the interaction between them. We can classify the electronic states as belonging to the electronic shells s, p, d etc.



The existence of a forbidden gap is not tied to the periodicity of the lattice! Amorphous materials can also display a band gap.

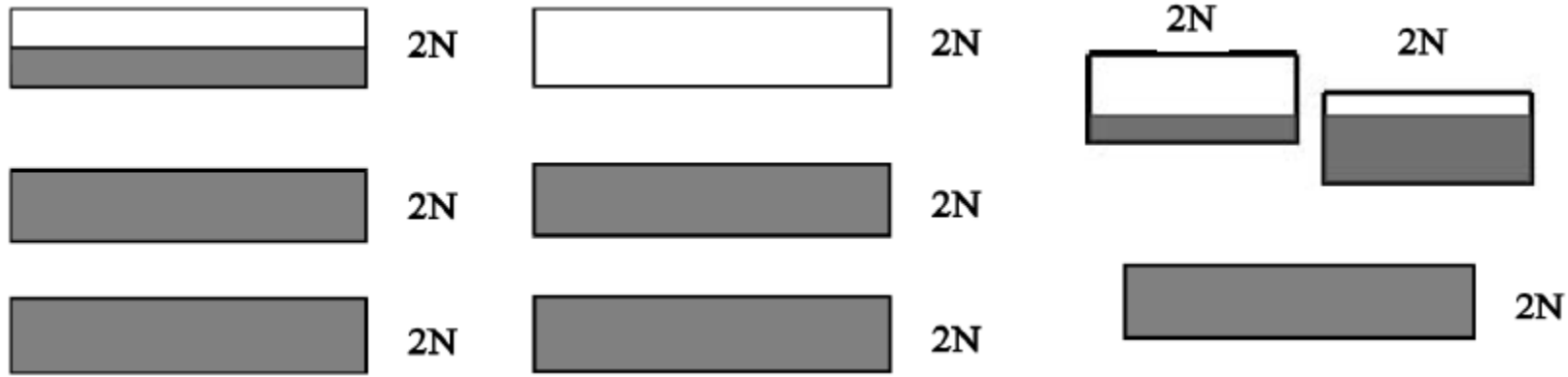
If a crystal with a primitive cubic lattice contains N atoms and thus N primitive unit cells, then an **atomic energy level E_i** of the free atom will split into N states (due to the interaction with the rest of $N - 1$ atoms).

Each band can be occupied by $2N$ electrons.

Fig. 1.1. Broadening of the energy levels as a large number of identical atoms from the first row of the periodic table approach one another (schematic). The separation r_0 corresponds to the approximate equilibrium separation of chemically bound atoms. Due to the overlap of the 2s and 2p bands, elements such as Be with two outer electrons also become metallic. Deep-lying atomic levels are only slightly broadened and thus, to a large extent, they retain their atomic character

Tight-Binding Approximation

If a crystal with a primitive cubic lattice contains N atoms and thus N primitive unit cells, then an **atomic energy level E_i** of the free atom will split into N states (due to the interaction with the rest of $N - 1$ atoms). **Each band can be occupied by $2N$ electrons.**



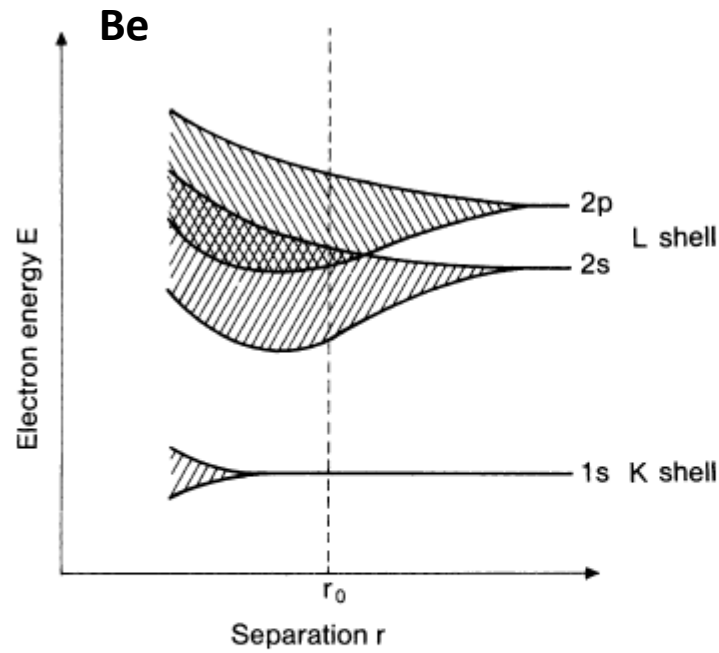
An odd number of electrons per cell (metal)

An even number of electrons per cell (non-metal)

An even number of electrons per cell but overlapping bands (metals of the II group, e.g. Be → next slide!)

Tight-Binding Approximation

The states can mix: for instance sp^3 hybridization.



H. Ibach, H. Lüth, Solid-State Physics

Fig. 1.1. Broadening of the energy levels as a large number of identical atoms from the first row of the periodic table approach one another (schematic). The separation r_0 corresponds to the approximate equilibrium separation of chemically bound atoms. Due to the overlap of the 2s and 2p bands, elements such as Be with two outer electrons also become metallic. Deep-lying atomic levels are only slightly broadened and thus, to a large extent, they retain their atomic character

C, Si, Ge

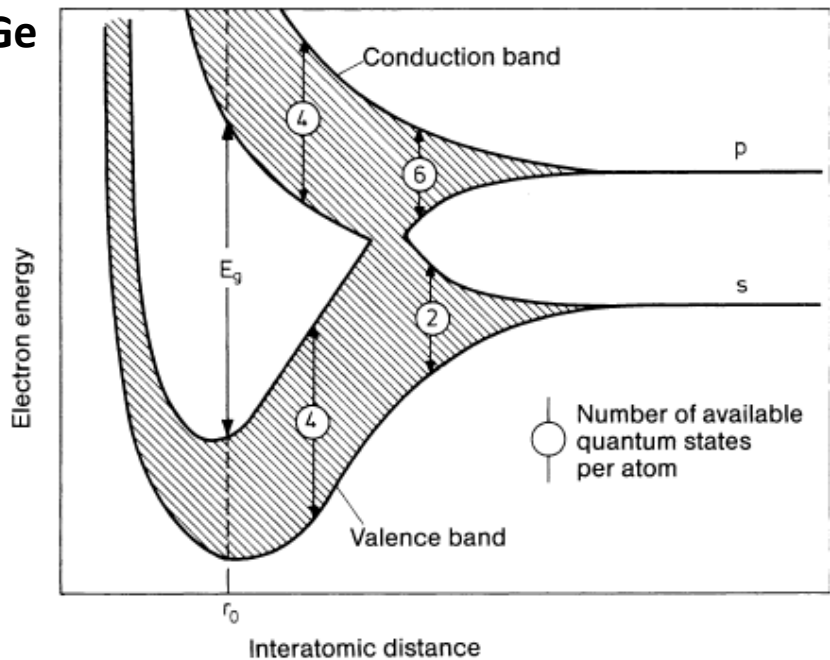


Fig. 7.9. Schematic behavior of the energy bands as a function of atomic separation for the tetrahedrally bound semiconductors diamond (C), Si, and Ge. At the equilibrium separation r_0 there is a forbidden energy gap of width E_g between the occupied and unoccupied bands that result from the sp^3 hybrid orbitals. For diamond, the sp^3 hybrid stems from the 2s and 2p³ atomic states, for Si from the 3s and 3p³, and for Ge from the 4s and 4p³. One sees from this figure that the existence of a forbidden energy region is not tied to the periodicity of the lattice. Thus amorphous materials can also display a band gap. (After [7.1])

Tight-Binding Approximation

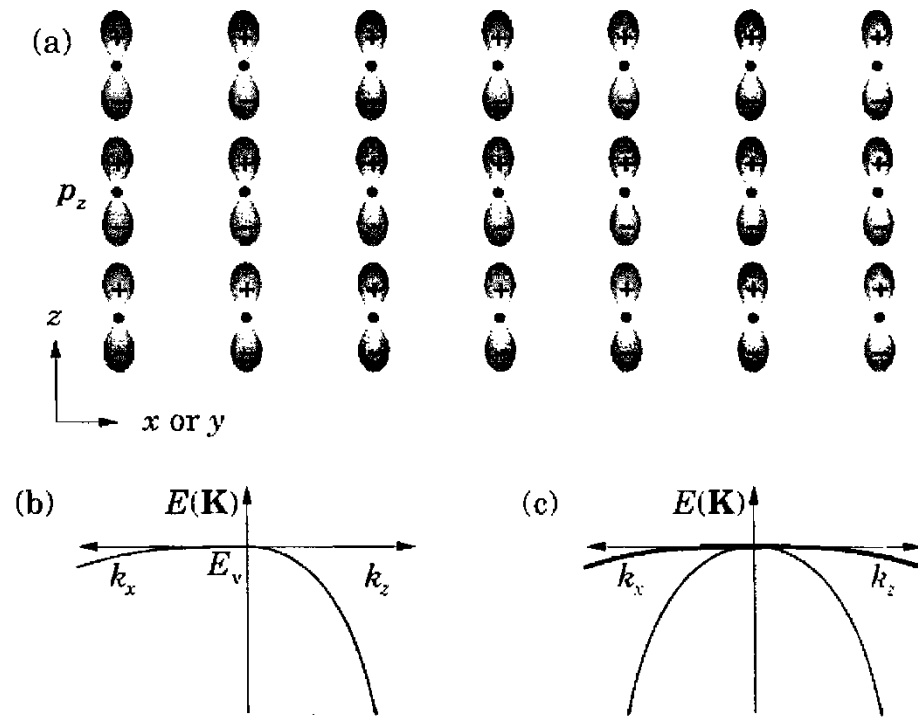


FIGURE 2.17. Valence bands constructed from p orbitals. (a) Lattice of p_z orbitals. (b) Band structure of the p_z orbitals only; the band is ‘light’ along k_z to the right and ‘heavy’ along k_x (or k_y) to the left. (c) Total bands from all three p orbitals, showing a doubly degenerate ‘heavy’ band and a single ‘light’ band.

Tight-Binding Approximation

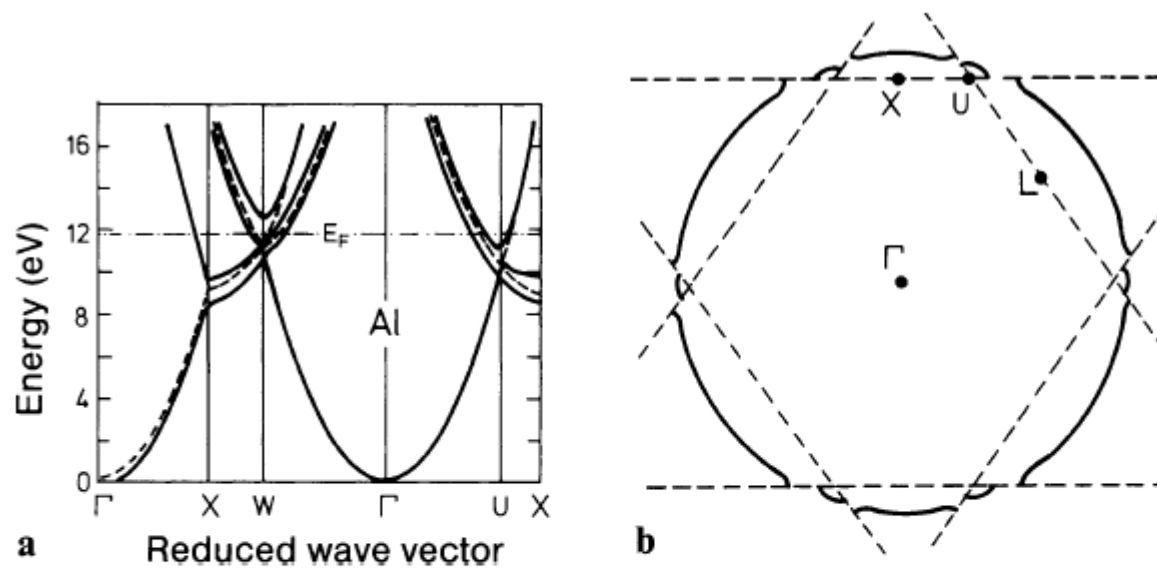


Fig. 7.11. (a) Theoretical bandstructure $E(\mathbf{k})$ for Al along directions of high symmetry (Γ is the center of the Brillouin zone). The dotted lines are the energy bands that one would obtain if the s - and p -electrons in Al were completely free (“empty” lattice). After [7.3]. (b) Cross section through the Brillouin zone of Al. The zone edges are indicated by the dashed lines. The Fermi “sphere” of Al (—) extends beyond the edges of the first Brillouin zone

Michał Baj

Fermi surfaces of metals

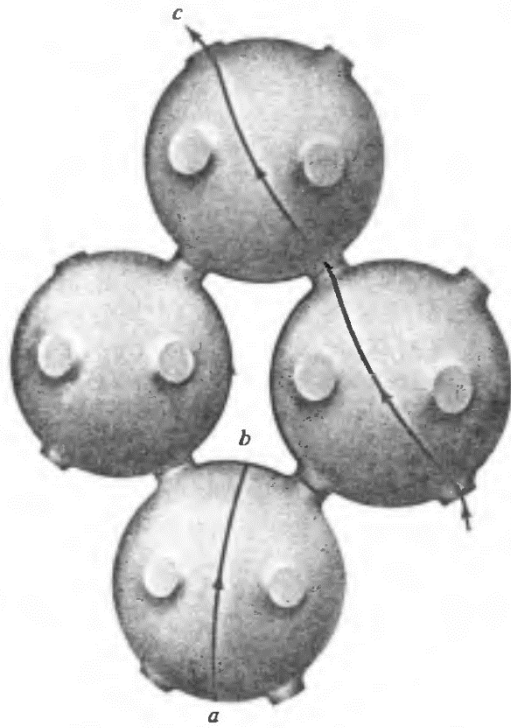


Figure 15.7

Indicating only a few of the surprisingly many types of orbits an electron can pursue in k -space when a uniform magnetic field is applied to a noble metal. (Recall that the orbits are given by slicing the Fermi surface with planes perpendicular to the field.) The figure displays (a) a closed particle orbit; (b) a closed hole orbit; (c) an open orbit, which continues in the same general direction indefinitely in the repeated-zone scheme.

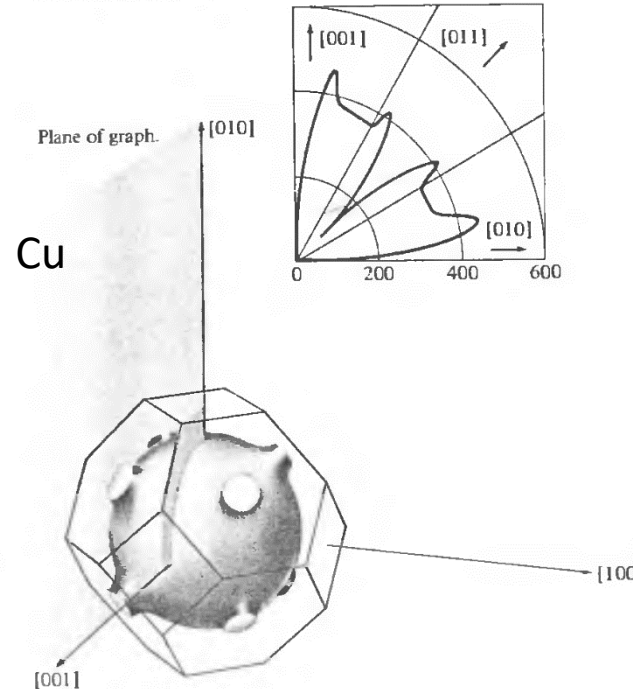


Figure 15.8

The spectacular direction dependence of the high-field magnetoresistance in copper that is characteristic of a Fermi surface supporting open orbits. The [001] and [010] directions of the copper crystal are as indicated in the figure, and the current flows in the [100] direction perpendicular to the graph. The magnetic field is in the plane of the graph. Its magnitude is fixed at 18 kilogauss, and its direction varied continuously from [001] to [010]. The graph is a polar plot of

$$\frac{\rho(H) - \rho(0)}{\rho(0)}$$

vs. orientation of the field. The sample is very pure and the temperature very low (4.2 K—the temperature of liquid helium) to insure the highest possible value for ω_{ct} . (J. R. Klauder and J. E. Kunzler, *The Fermi Surface*, Harrison and Webb, Inc., Wiley, New York, 1960.)

Fermi surfaces of metals

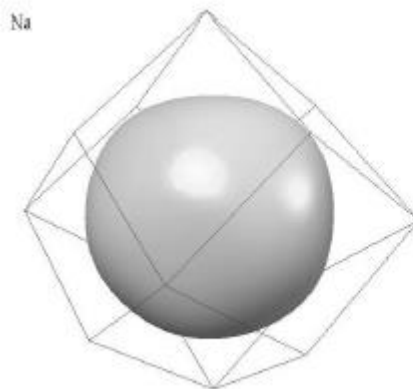


Fig.10 Fermi surface of sodium.

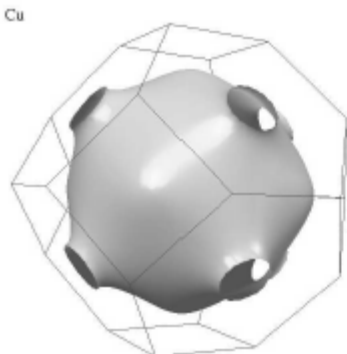


Fig. 11 In the three noble metals the free electron sphere bulges out in the [111] directions to make contact with the hexagonal zone faces.

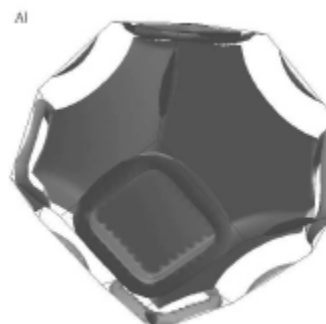


Fig.13 Fermi surface of aluminum

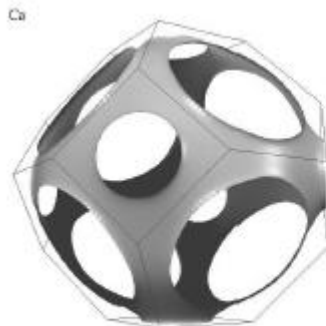


Fig.12 Fermi surface of calcium

Fermi surfaces of metals

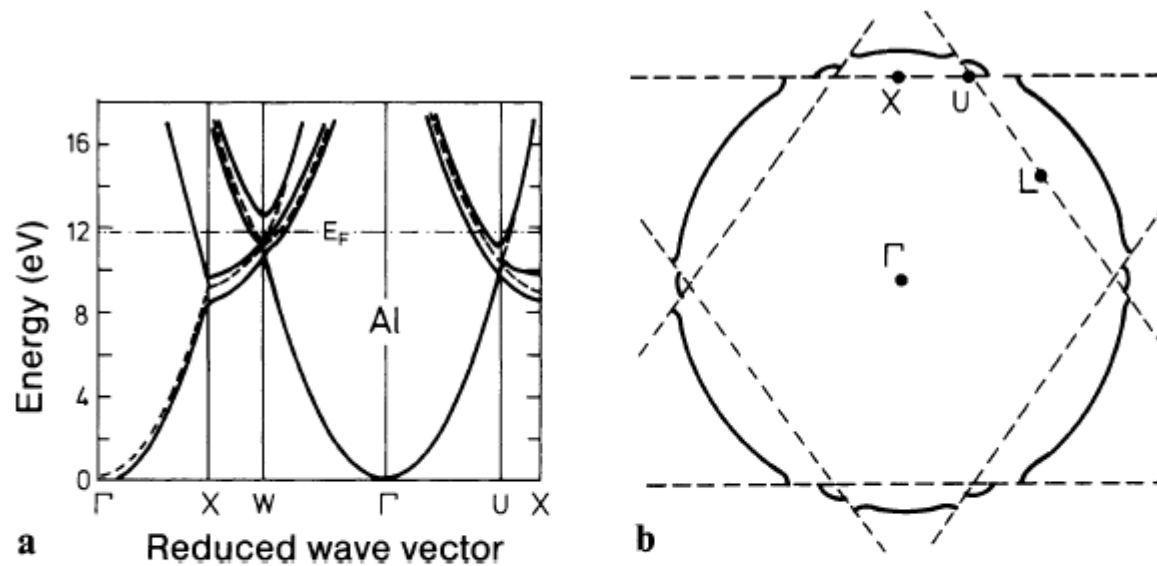


Fig. 7.11. (a) Theoretical bandstructure $E(k)$ for Al along directions of high symmetry (Γ is the center of the Brillouin zone). The dotted lines are the energy bands that one would obtain if the s - and p -electrons in Al were completely free (“empty” lattice). After [7.3]. (b) Cross section through the Brillouin zone of Al. The zone edges are indicated by the dashed lines. The Fermi “sphere” of Al (—) extends beyond the edges of the first Brillouin zone

Michał Baj

Tight-Binding Approximation

PHYSICAL REVIEW

VOLUME 116, NUMBER 3

NOVEMBER 1, 1959

Fermi Surface in Aluminum

WALTER A. HARRISON

General Electric Research Laboratory, Schenectady, New York

(Received June 15, 1959)

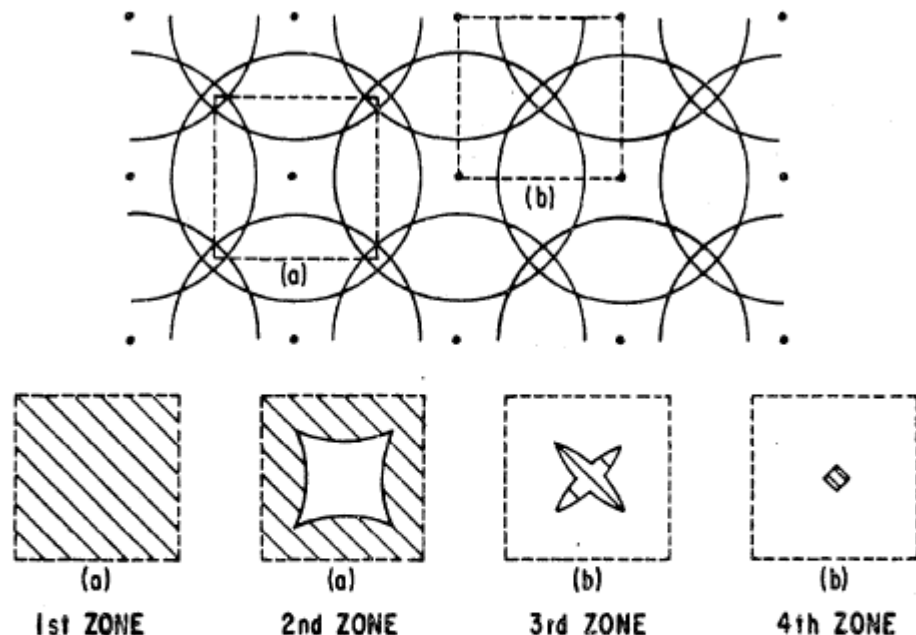


FIG. 1. Schematic determination of the free-electron Fermi "surface" in a two-dimensional square lattice. The diagram above indicates free-electron "spheres" drawn around each reciprocal lattice point; the dashed squares (a) and (b) represent two choices of Brillouin zones used in the drawings below. The cross-hatched areas below correspond to regions occupied by electrons.

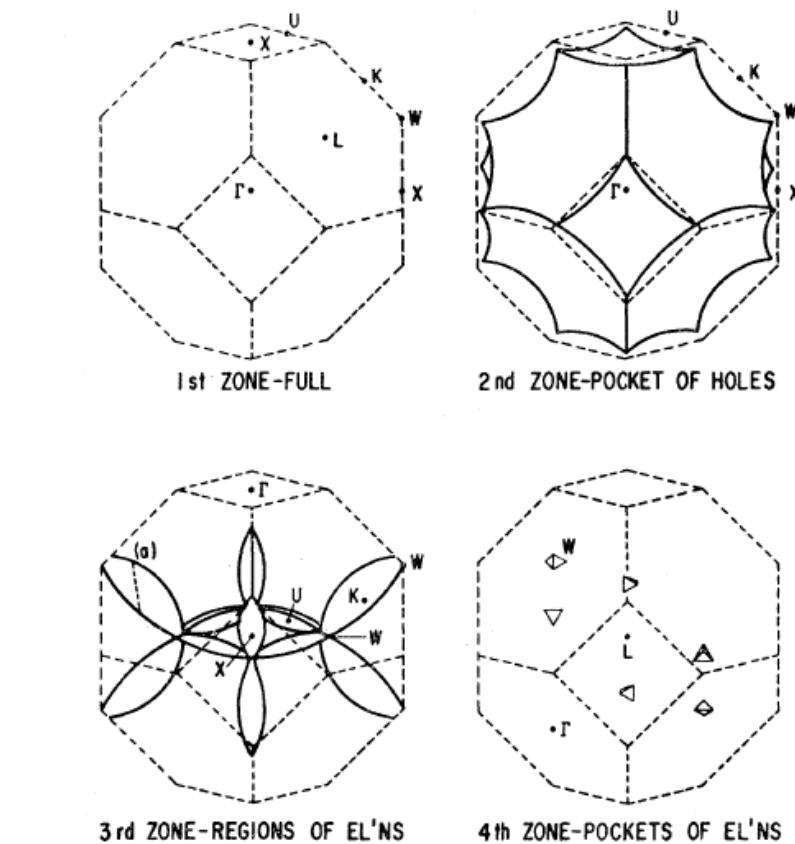


FIG. 2. Free-electron Fermi surface in aluminum, constructed in a manner analogous to that indicated in Fig. 1. Various symmetry points are specified in each zone; points K and U are equivalent. The dotted curve (a) corresponds to an electron orbit in wave-number space corresponding to a particular orientation of magnetic field discussed in the text.

Tight-Binding Approximation

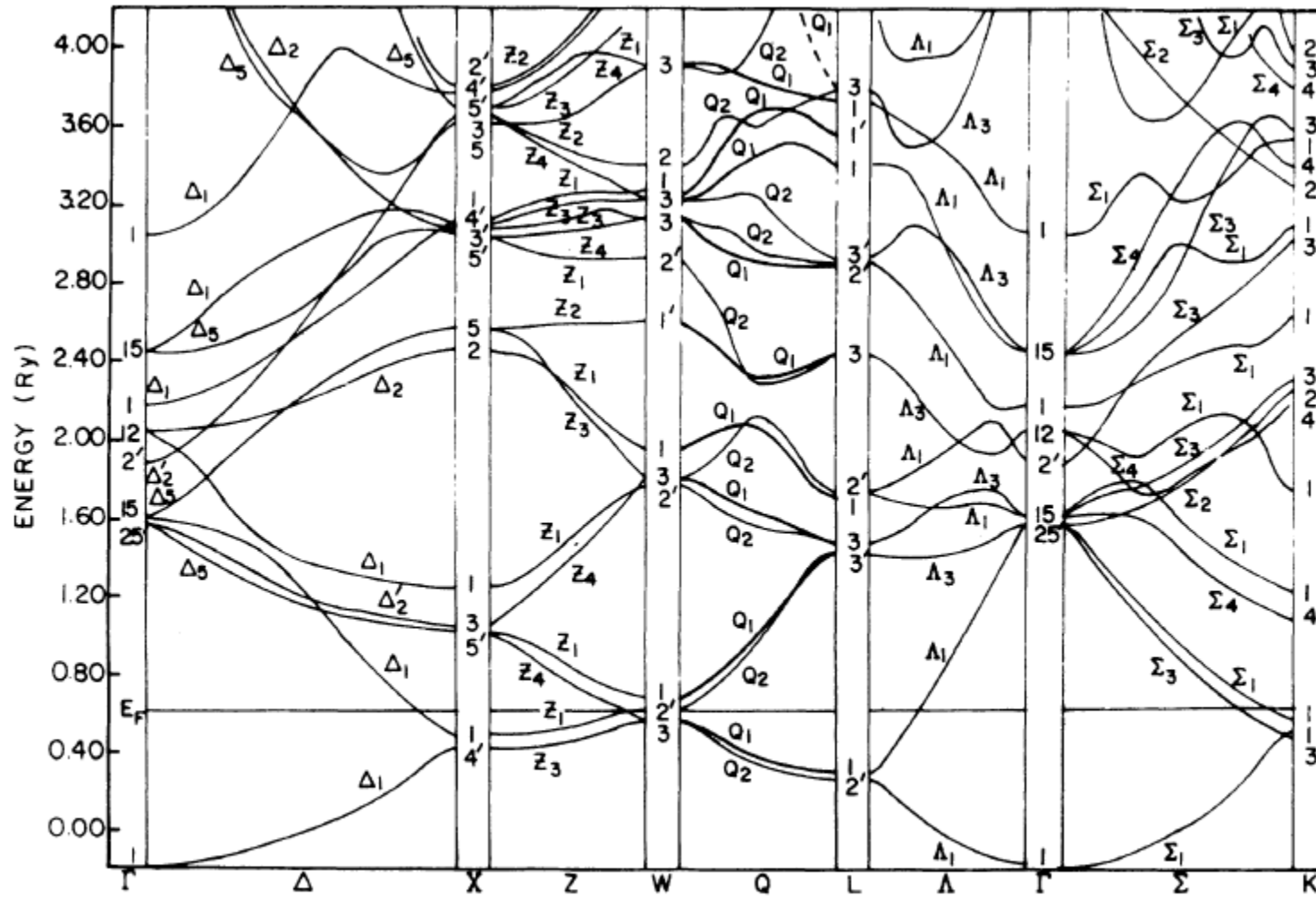


FIG. 1. Electronic structure of Al along symmetry directions.

Michał Baj

Tight-Binding Approximation

Szmulowicz, F., Segall, B.: Phys. Rev. B21, 5628 (1980).

Tutaj 08.10.2014

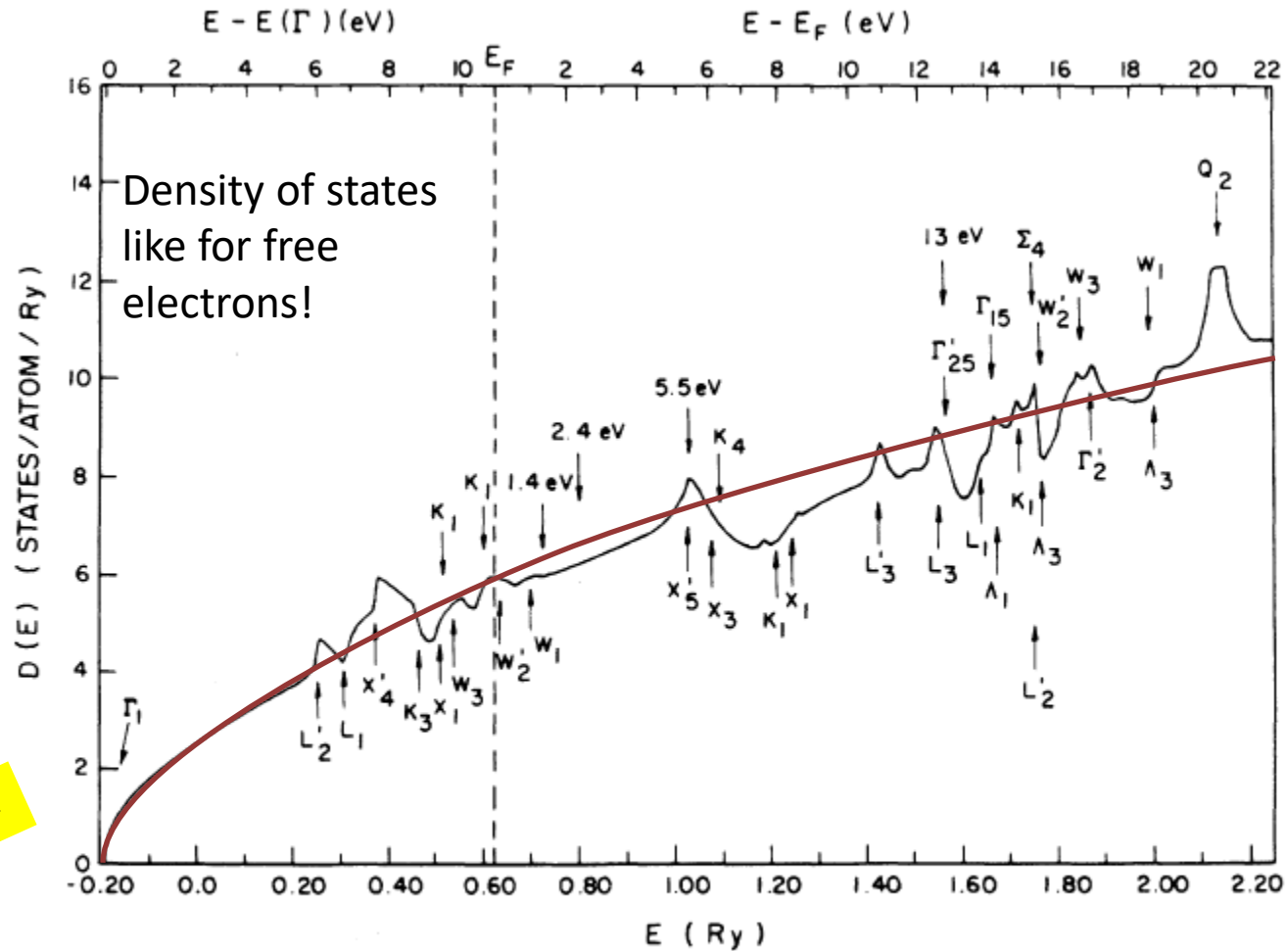


FIG. 2. Density of states of Al. The states responsible for structure are indicated by letters denoting their irreducible representations. The arrows at 1.4, 2.4, 5.5, and 13 eV indicate the location of structure in the experimental K absorption in Ref. 6.

Michał Baj

Tight-Bind

Cu: $[1s^2 2s^2 2p^6 3s^2 3p^6] 3d^{10} 4s^1$
[Ar] $3d^{10} 4s^1$

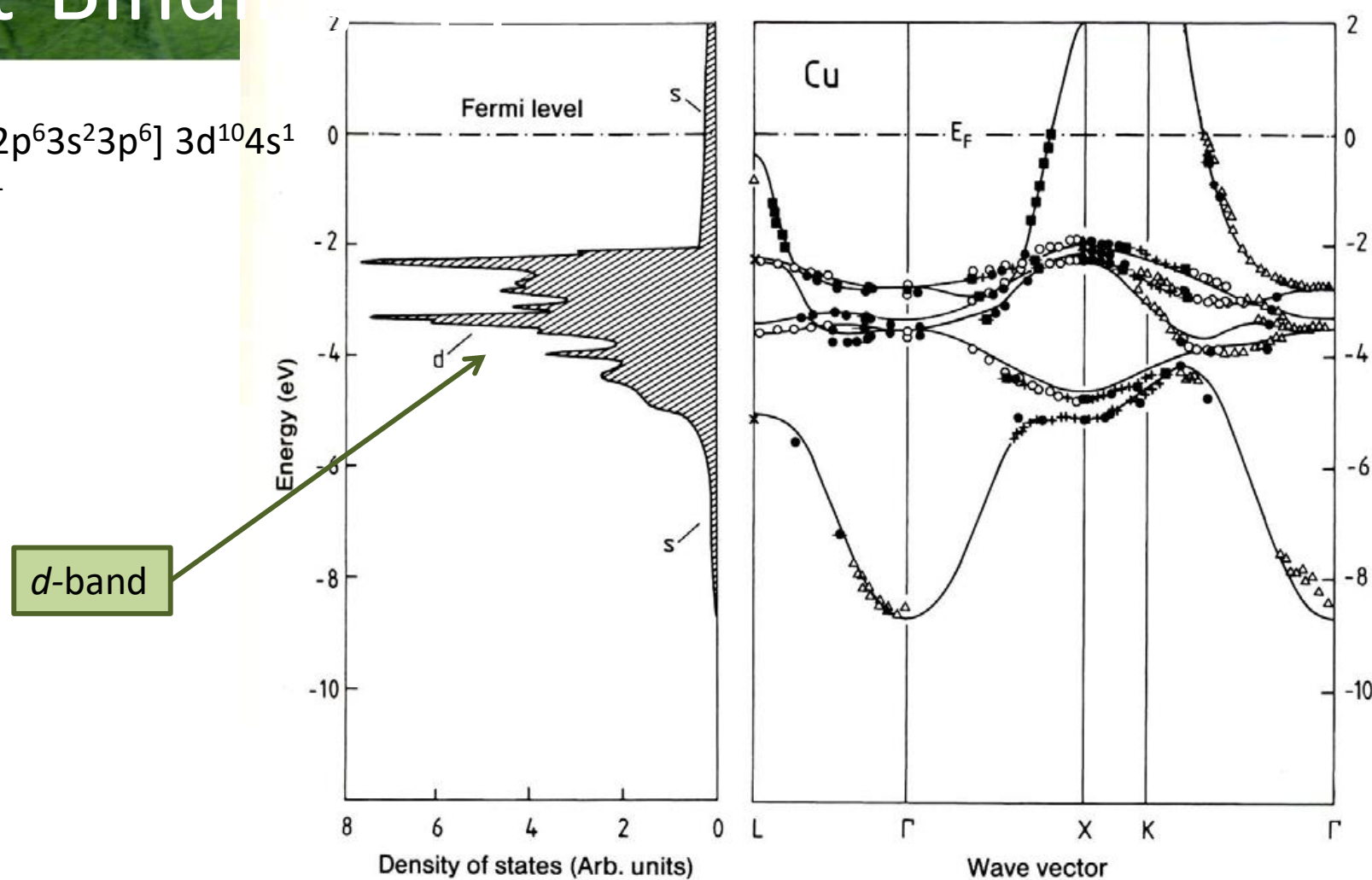
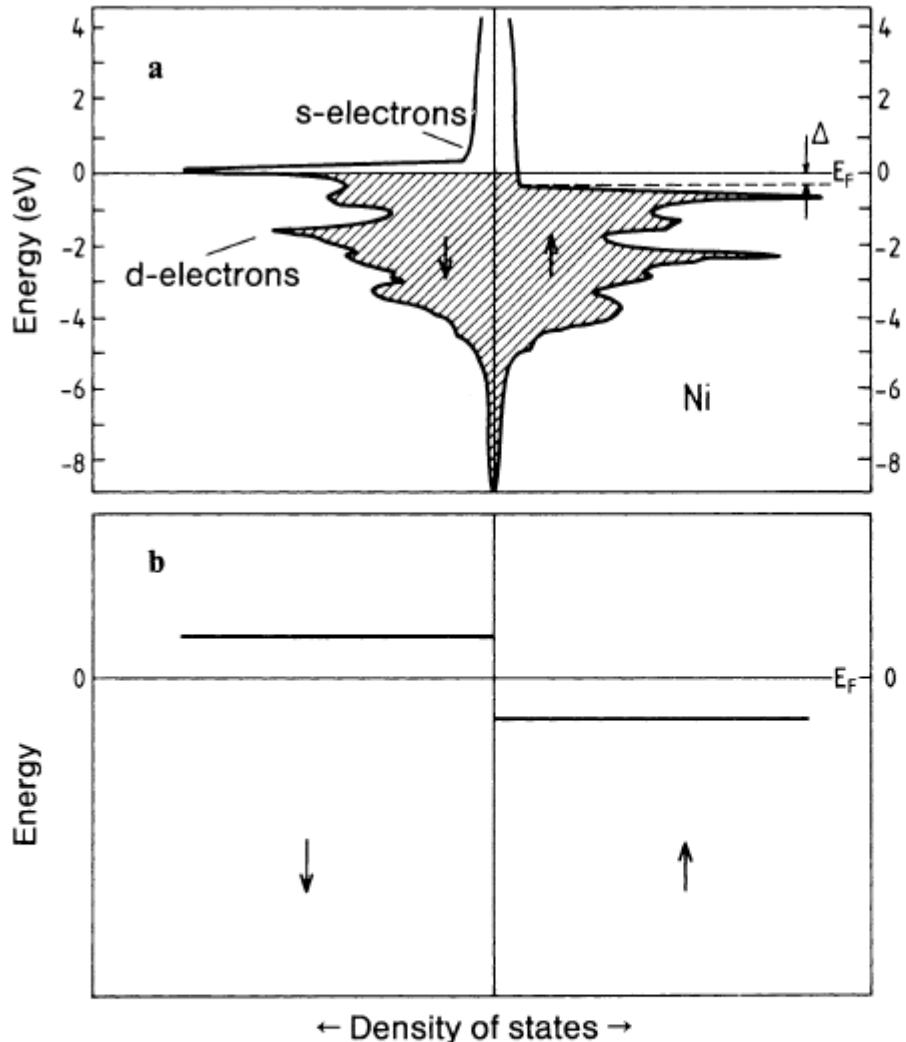


Fig. 7.12. Bandstructure $E(\mathbf{k})$ for copper along directions of high crystal symmetry (right). The experimental data were measured by various authors and were presented collectively by Courths and Hüfner [7.4]. The full lines showing the calculated energy bands and the density of states (left) are from [7.5]. The experimental data agree very well, not only among themselves, but also with the calculation



Ni: [1s²2s²2p⁶3s²3p⁶] 3d⁹4s¹ [Ar] 3d⁹4s¹
ferromagnetic ordering, exchange interaction, different energies for different spins, two different densities of states for two spins \uparrow and \downarrow

Δ – Stoner gap

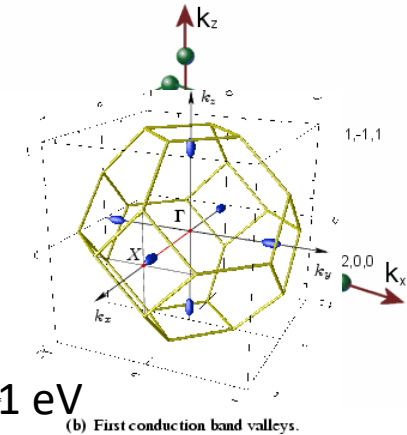
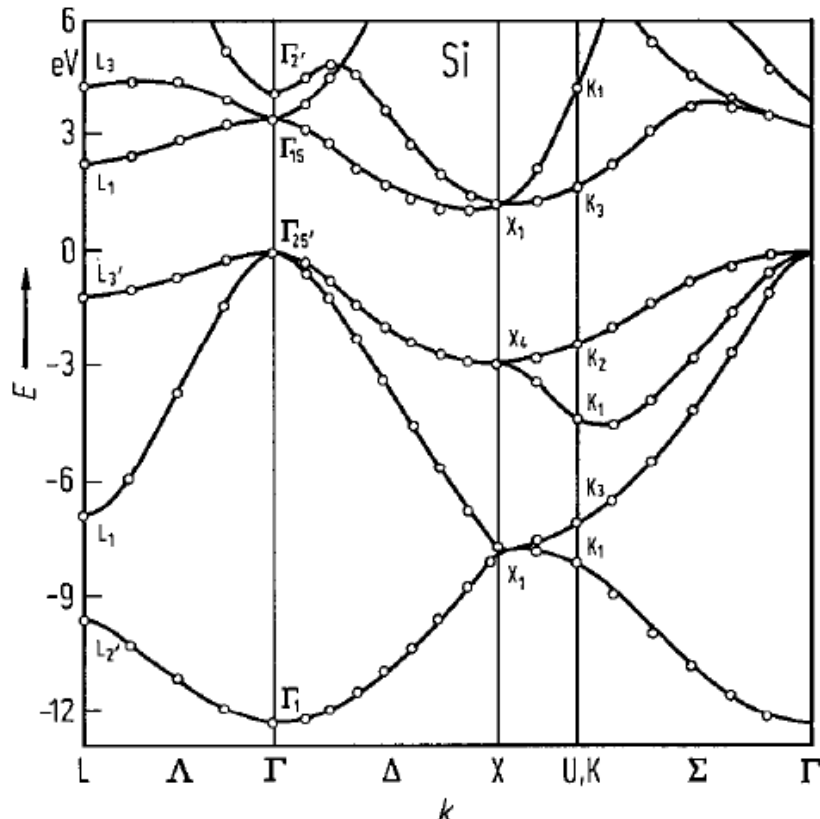
Fig. 8.6. (a) Calculated density of states of nickel (after [8.3]). The exchange splitting is calculated to be 0.6 eV. From photoelectron spectroscopy a value of about 0.3 eV is obtained. However the values cannot be directly compared, because a photoemitted electron leaves a hole behind, so that the solid remains in an excited state. The distance Δ between the upper edge of the d-band of majority spin electrons and the Fermi energy is known as the Stoner gap. In the bandstructure picture, this is the minimum energy for a spin flip process (the s-electrons are not considered in this treatment). (b) A model density of states to describe the thermal behavior of a ferromagnet

Semiconductors

Semiconductors of the group IV (Si, Ge) –diamond structure

Semiconductors Al₃IBV (e.g. GaAs, GaN) i Al₂BVI (np. ZnTe, CdSe) – zinc-blend or wurtzite structure

Semiconductors AlVBVI (np. SnTe, PbSe) –NaCl structure



Conduction band minima in Δ point, constant energy surfaces – ellipsoids (6 pieces), $m//=0,92 m_0$, $m\perp=0,19 m_0$,

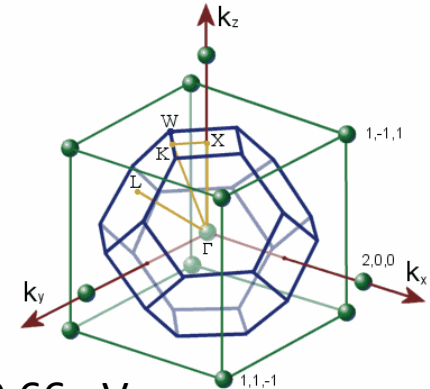
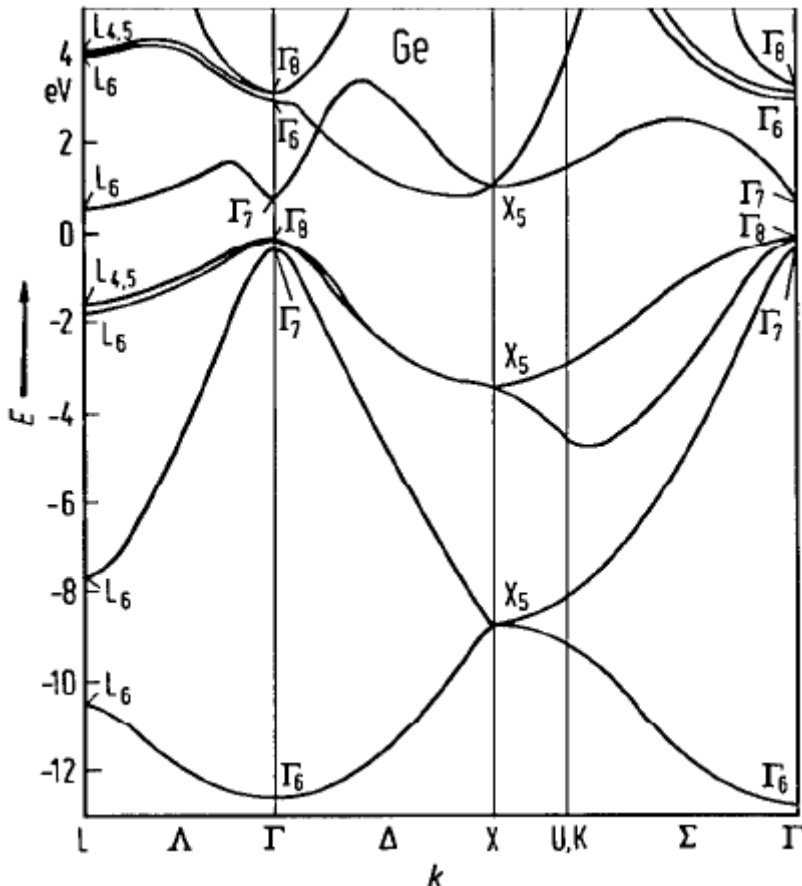
The maximum of the valence band in Γ point, $m/h=0,153 m_0$, $m/hh=0,537 m_0$, $m/so=0,234 m_0$, $\Delta/so= 0,043 \text{ eV}$

Semiconductors

Semiconductors of the group IV (Si, Ge) –diamond structure

Semiconductors Al₃IBV (e.g. GaAs, GaN) i Al₂BVI (np. ZnTe, CdSe) – zinc-blend or wurtzite structure

Semiconductors AlVBVI (np. SnTe, PbSe) –NaCl structure



Ge

Indirect bandgap, $Eg = 0,66$ eV

The maximum of the valence band in Γ point,
 $m\parallel h=0,04$ m0, $mhh=0,3$ m0, $mso=0,09$ m0,
 $\Delta so= 0,29$ eV

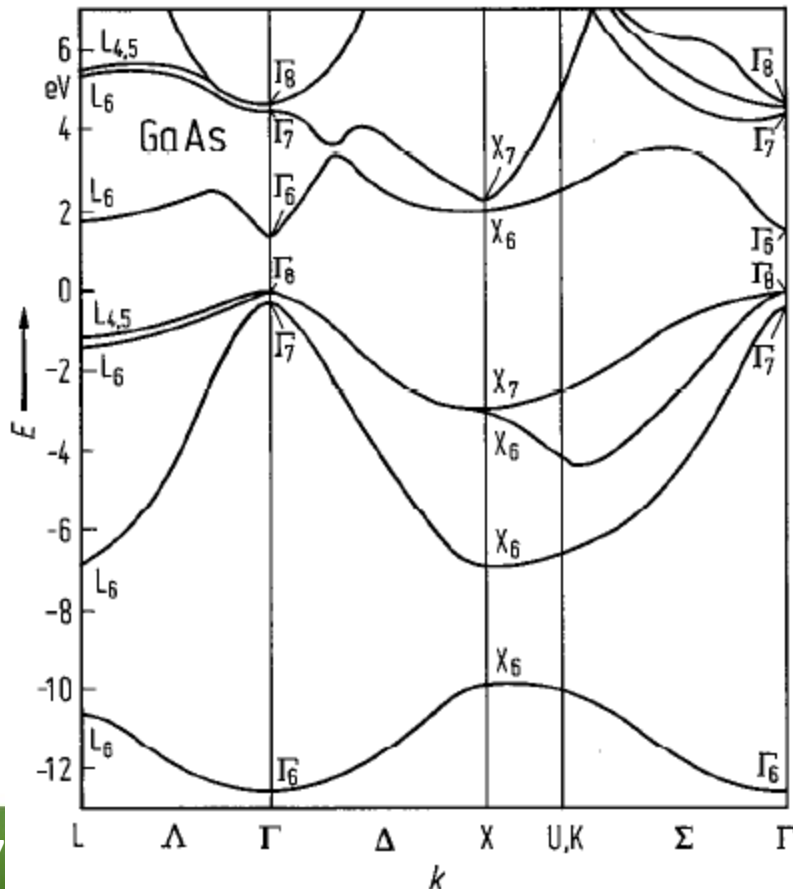
Conduction band minima in Δ point, constant
energy surfaces – ellipsoids (8 pieces), $m\parallel / = 1,6$
m0, $m\perp = 0,08$ m0,

Semiconductors

Semiconductors of the group IV (Si, Ge) –diamond structure

Semiconductors Al₃IBV (e.g. GaAs, GaN) i Al₂BVI (np. ZnTe, CdSe) – zinc-blend or wurtzite structure

Semiconductors AlVBVI (np. SnTe, PbSe) –NaCl structure

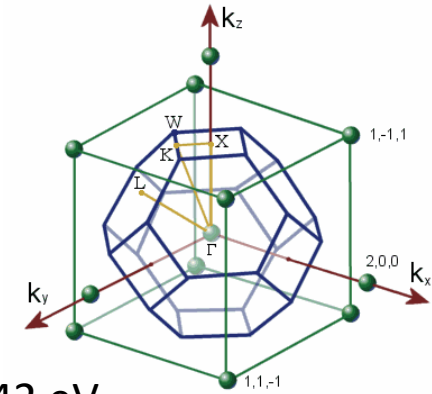


GaAs

Direct bandgap, $Eg = 1,42$ eV

The maximum of the valence band in Γ point,
 $mIh=0,076\text{ }m0$, $mhh=0,5\text{ }m0$, $mso=0,145\text{ }m0$,
 $\Delta so= 0,34\text{ eV}$

The minimum of the conduction band in Γ point,
constant energy surfaces – spheres,
 $mc=0,065\text{ }m0$

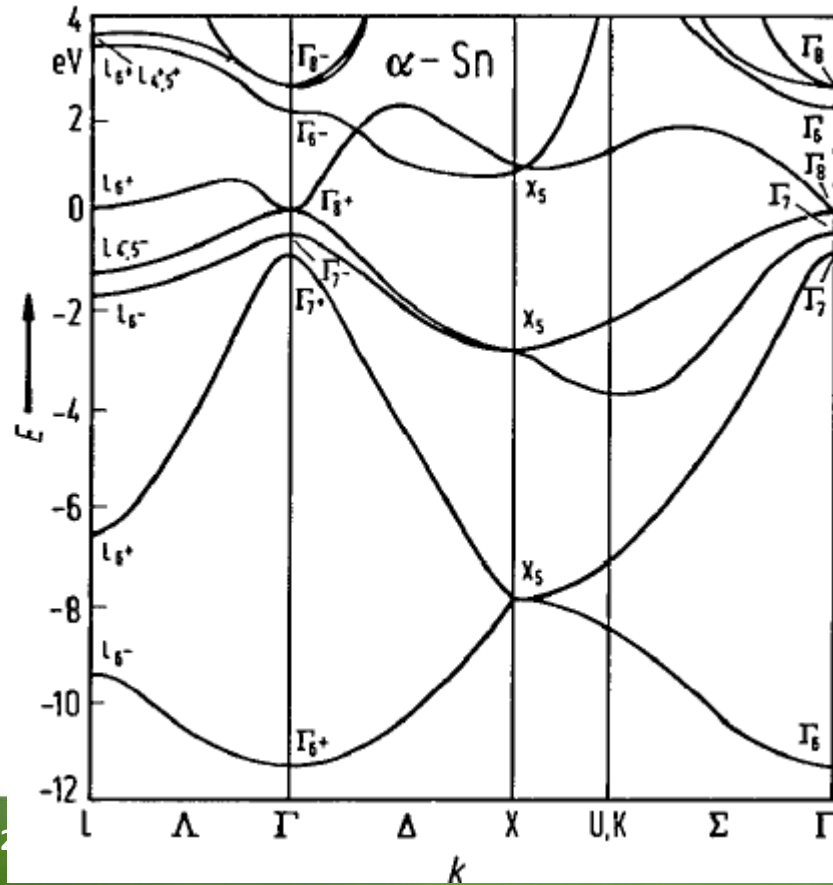


Semiconductors

Semiconductors of the group IV (Si, Ge) –diamond structure

Semiconductors Al₃IBV (e.g. GaAs, GaN) i Al₂IBVI (np. ZnTe, CdSe) – zinc-blend or wurtzite structure

Semiconductors Al₃VBVI (np. SnTe, PbSe) –NaCl structure



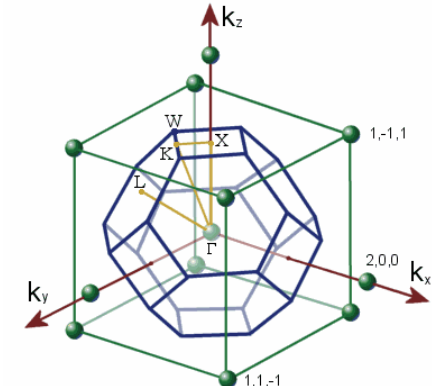
α -Sn

Diamond structure

Zero energy gap, $Eg = 0$ eV (inverted band-structure)

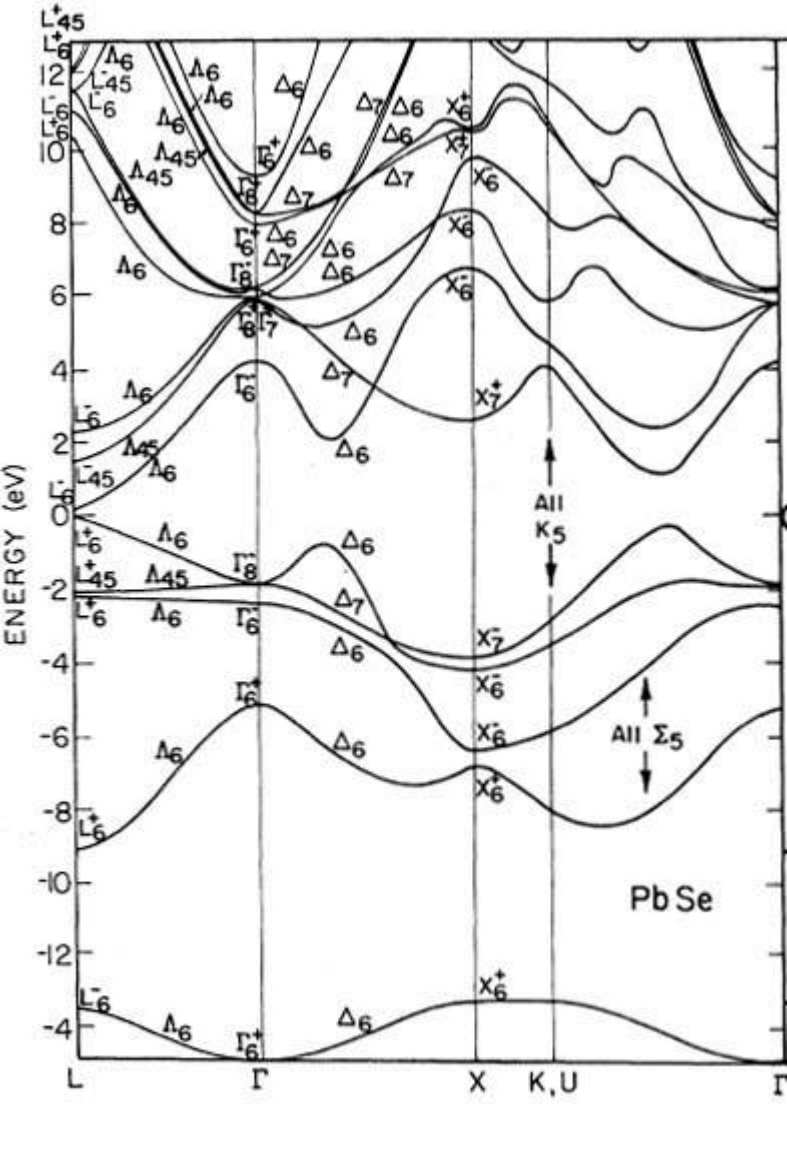
The maximum of the valence band in Γ point,
 $mv=0,195 m_0$, $mv2=0,058 m_0$, $\Delta so=0,8$ eV

The minimum of the conduction band in Γ point,
constant energy surfaces – spheres,
 $mc=0,024 m_0$



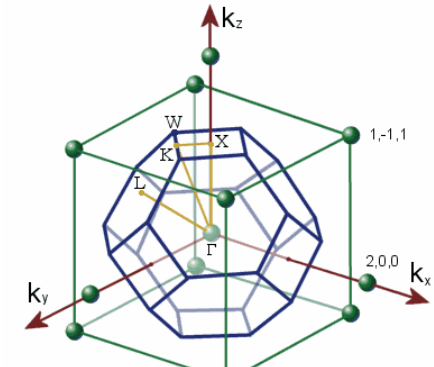
Semiconductors

Semiconductors of the group IV (Si, Ge) –diamond structure



i AlIBVI (np. ZnTe, CdSe) – zinc-blend or wurtzite

) –NaCl structure



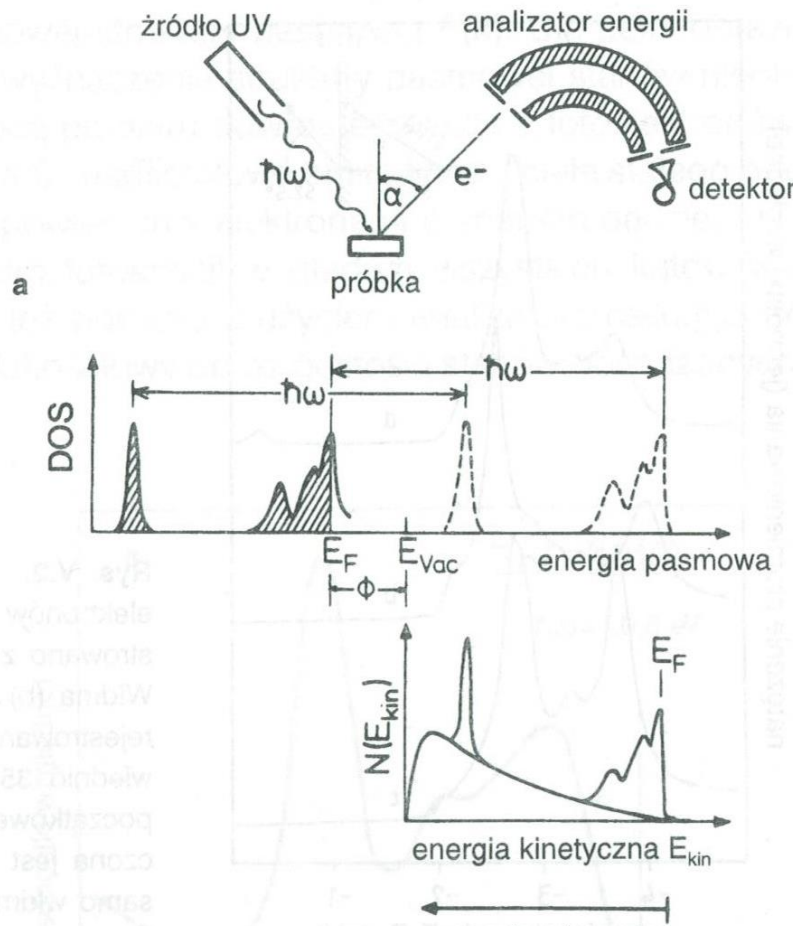
PbSe

Direct bandgap in *L-point*, $Eg = 0,28$ eV

The maximum of the valence band in *L point*,
constant energy surfaces – ellipsoids ,
 $m//=0,068 m_0$, $m\perp=0,034 m_0$,

The minimum of the conduction band in *L point*,
constant energy surfaces – ellipsoids $m//=0,07$
 m_0 , $m\perp=0,04 m_0$,

Photoemission spectroscopy



$$\hbar\omega = \phi + E_{kin} + E_b$$

work function

potential barrier

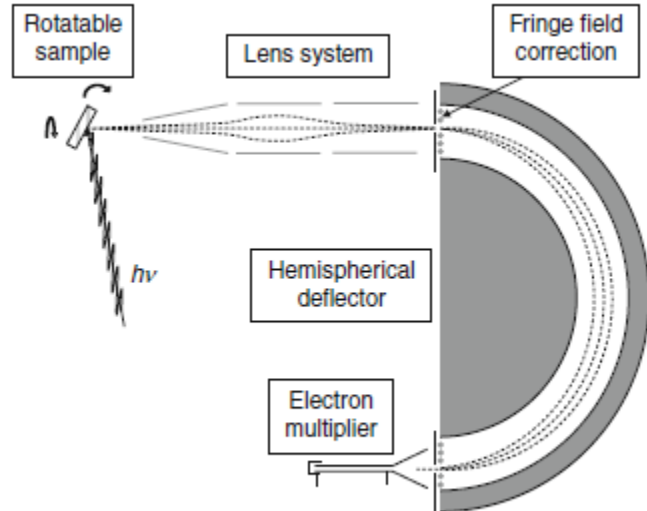


Fig. V.1. Experimental setup for photoemission spectroscopy

Photoemission spectroscopy

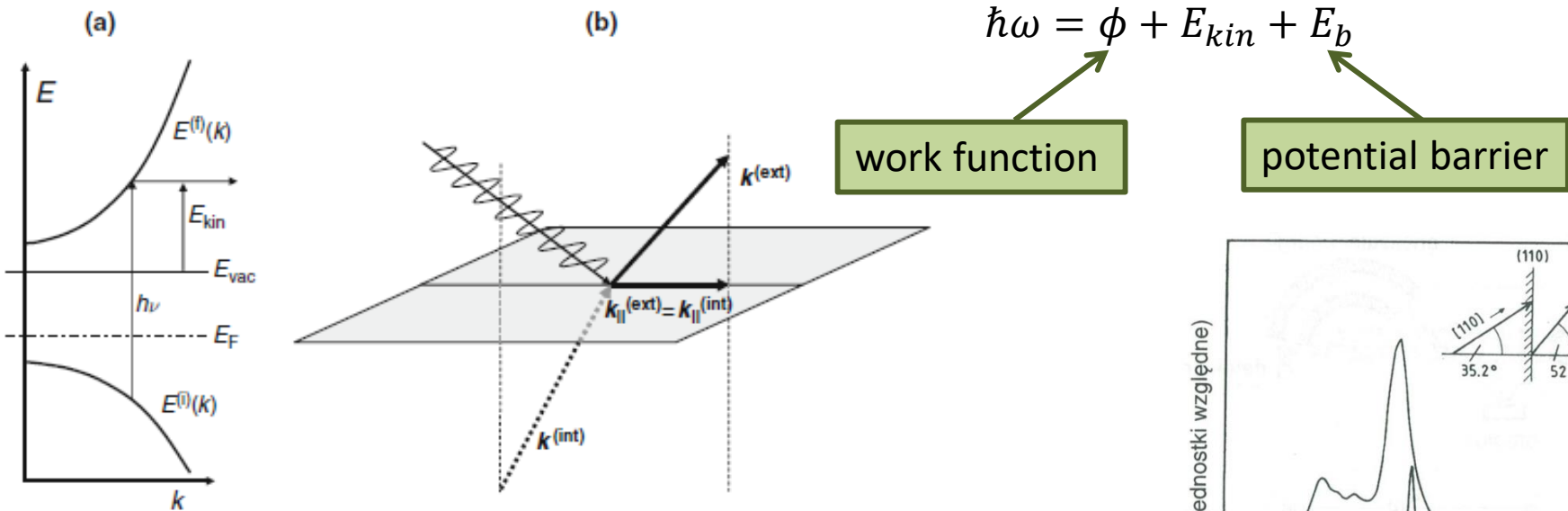
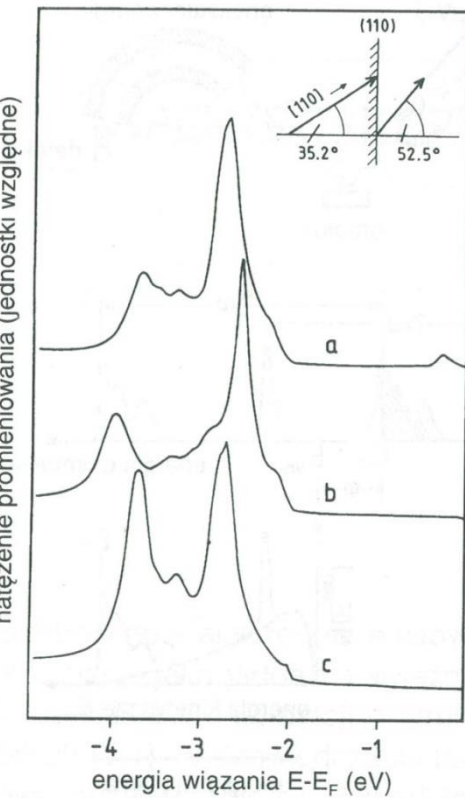
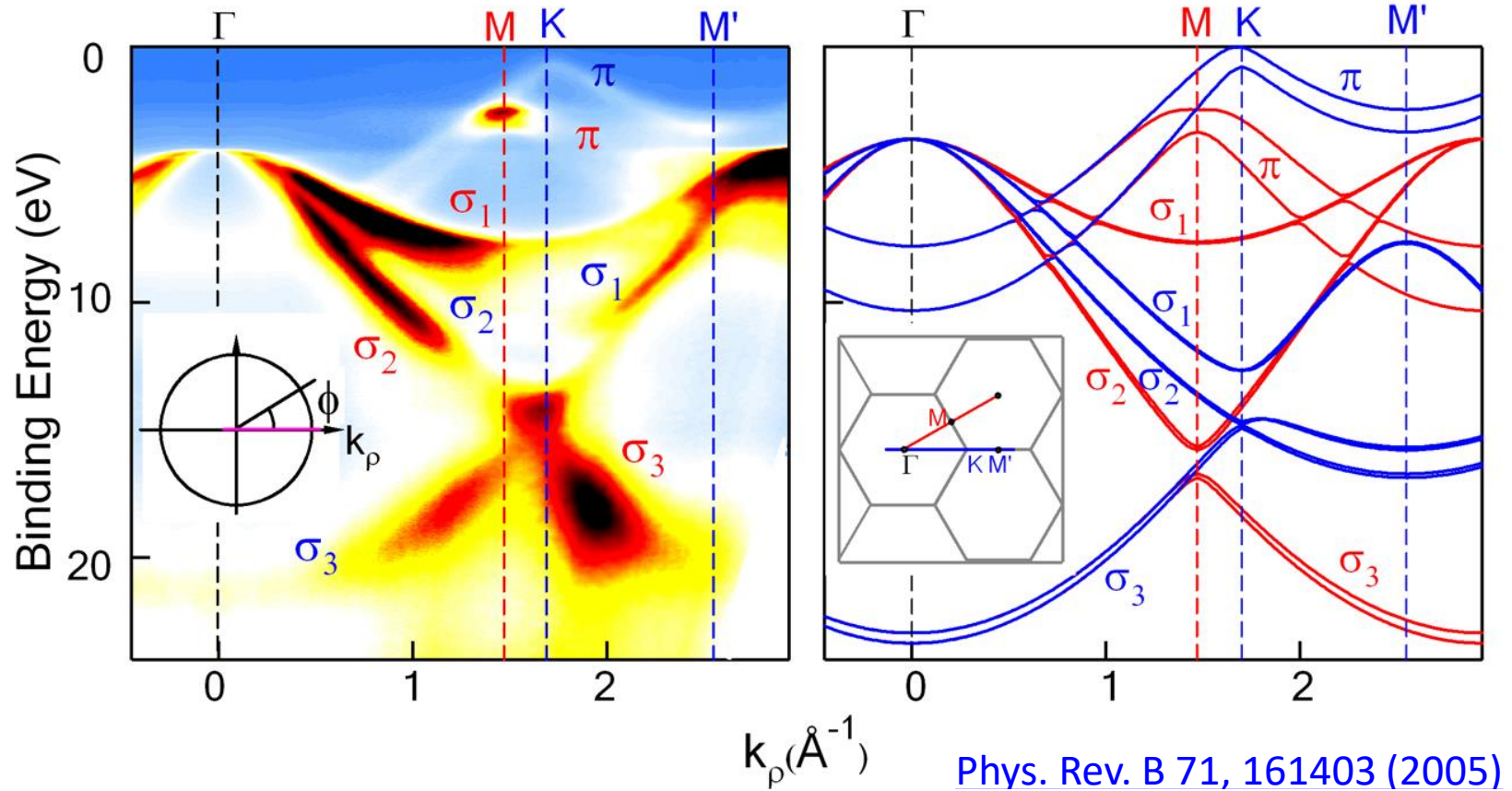


Fig. V.3. Illustration of the photoemission process. (a) A photon of energy $h\nu$ excites an electron from the initial state $E^{(i)}(k)$ to the final state $E^{(f)}(k)$ above the vacuum level E_{vac} . The kinetic energy of the photoemitted electron is $E_{kin} = E^{(f)}(k) - E_{vac}$. (b) The wave vectors of the electron inside $\mathbf{k}^{(int)}$ and outside $\mathbf{k}^{(ext)}$ have the same parallel components since the spatial phase $i\mathbf{r}_{\parallel}\mathbf{k}_{\parallel}$ has to be identical to make the wave function continuous at any given point \mathbf{r}_{\parallel} of the surface

Rys. V.2. Pomiar rozkładu kątowego widma fotoelektronów z powierzchni miedzi. Widmo (a) zarejestrowano z powierzchni Cu(111) w kierunku [111]. Widma (b) i (c) pochodzą z powierzchni Cu(110) i rejestrowane były pod kątami biegunkowymi odpowiednio $35,2^\circ$ i $52,5^\circ$. Wielkość wektora \mathbf{k} stanu początkowego odpowiadającego widmu (a) wyznaczona jest przez rzut wektora \mathbf{k} , dla którego takie samo widmo rejestrowane jest z powierzchni (110) (wg [V.2]).

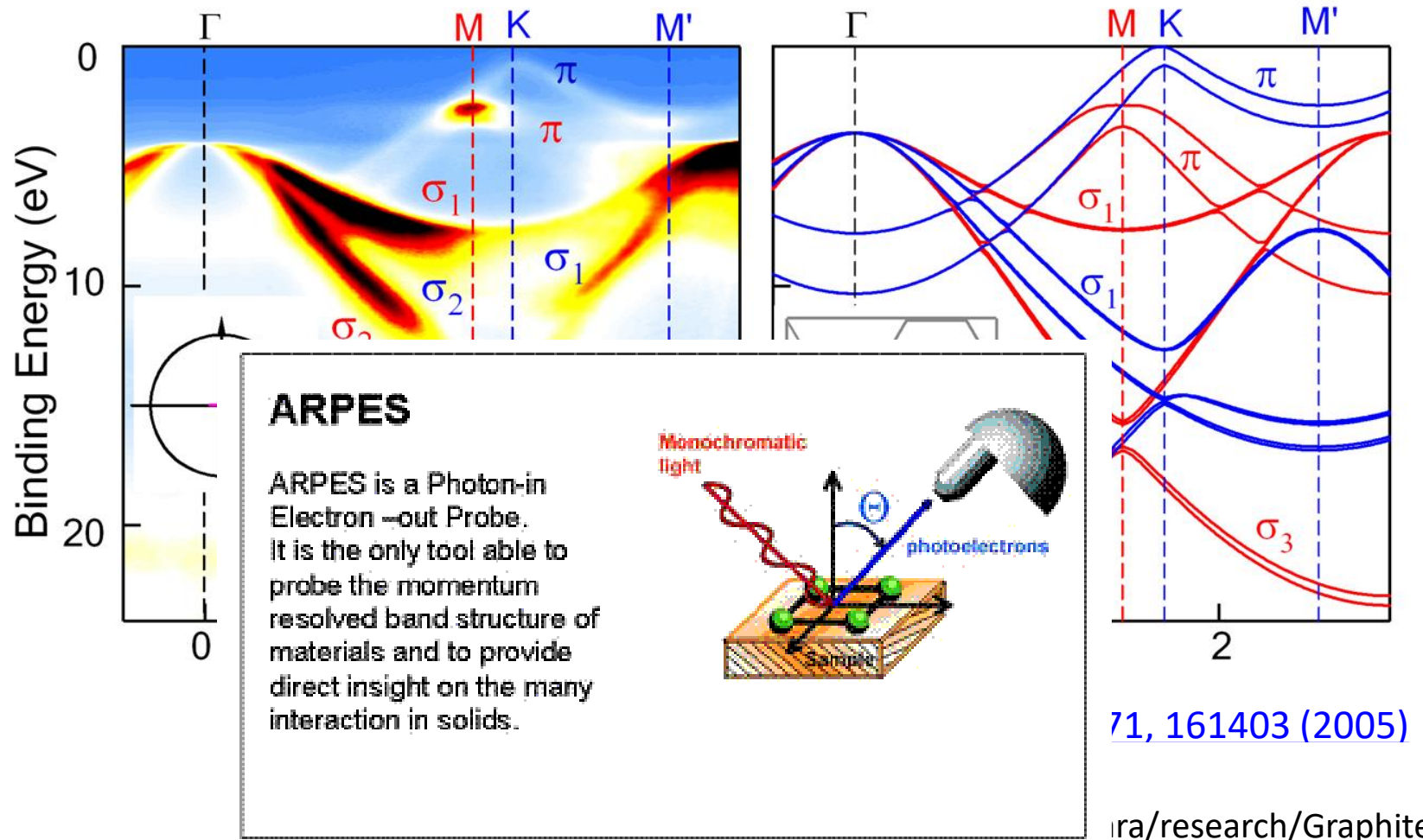


Photoemission spectroscopy



<http://www.physics.berkeley.edu/research/lanzara/research/Graphite.html>

Photoemission spectroscopy



Semiconductor heterostructures

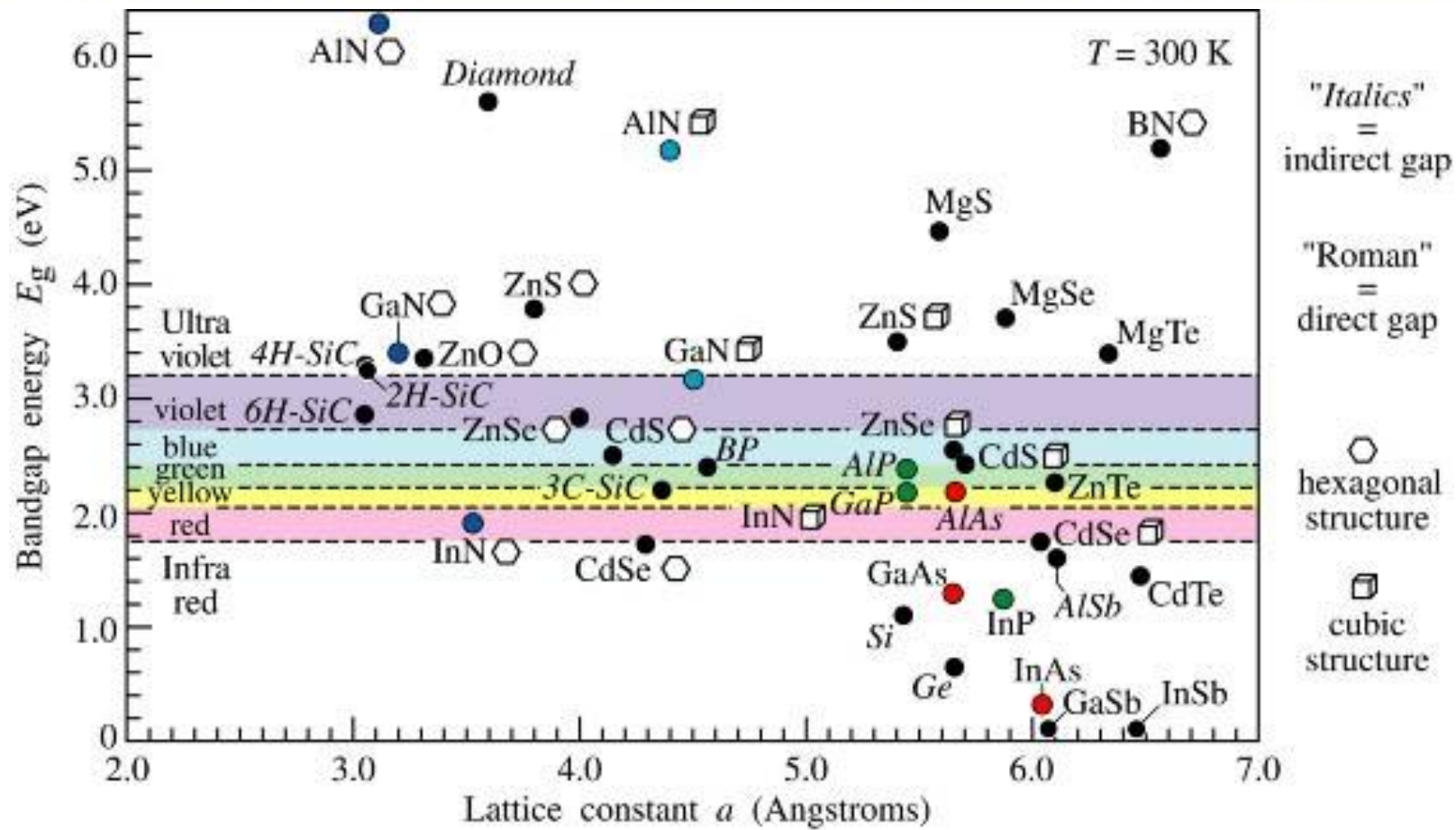
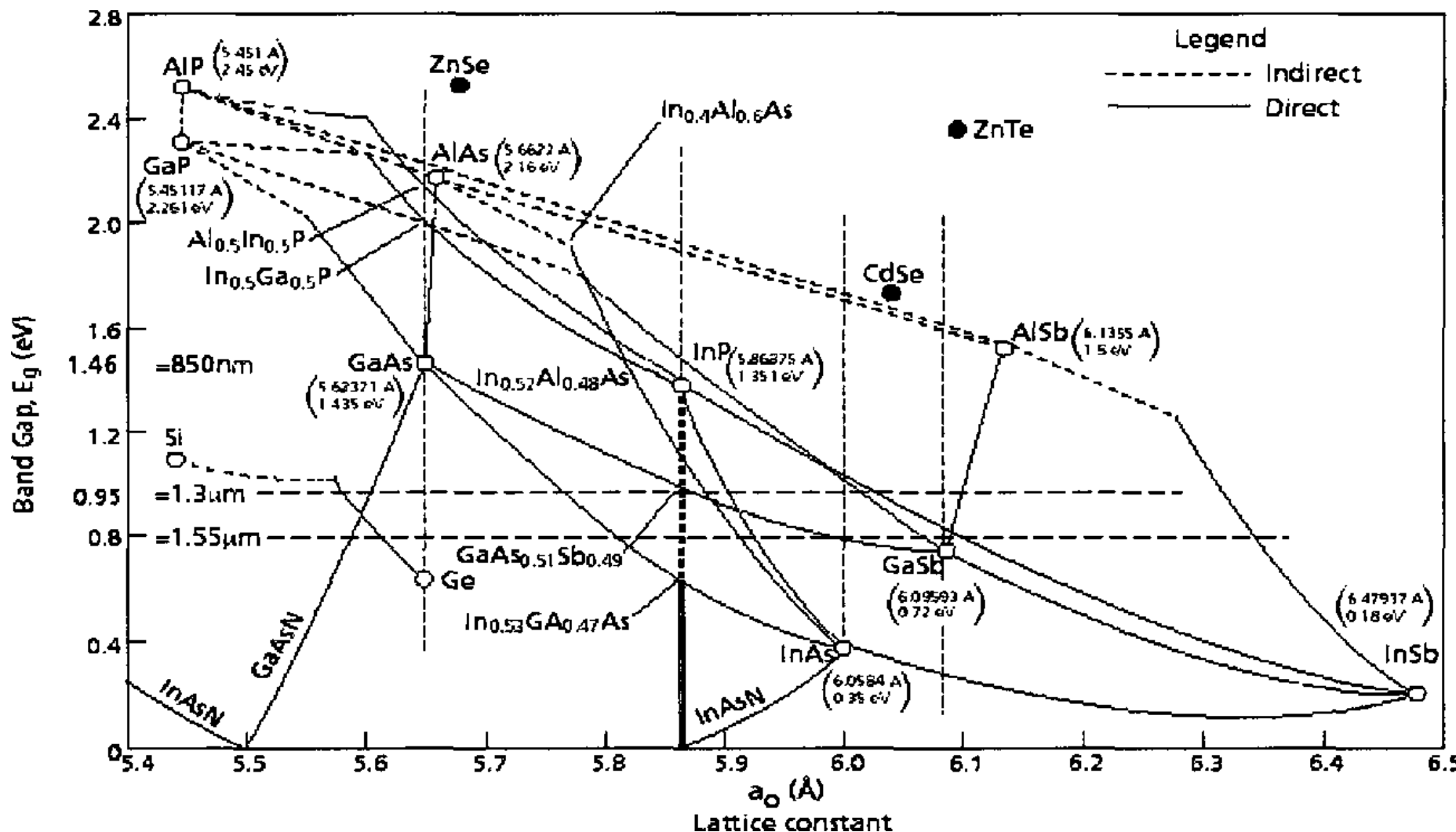


Fig. 11.4. Room-temperature bandgap energy versus lattice constant of common elemental and binary compound semiconductors.

Semiconductor heterostructures

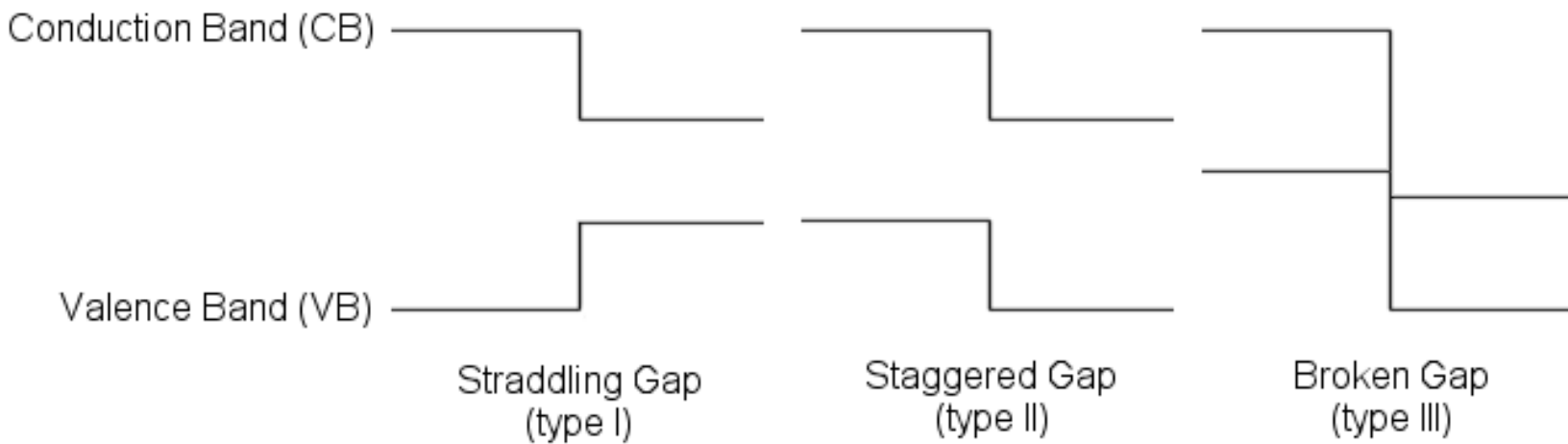


Investigation of high antimony-content gallium arsenic nitride-gallium arsenic antimonide heterostructures for long wavelength application

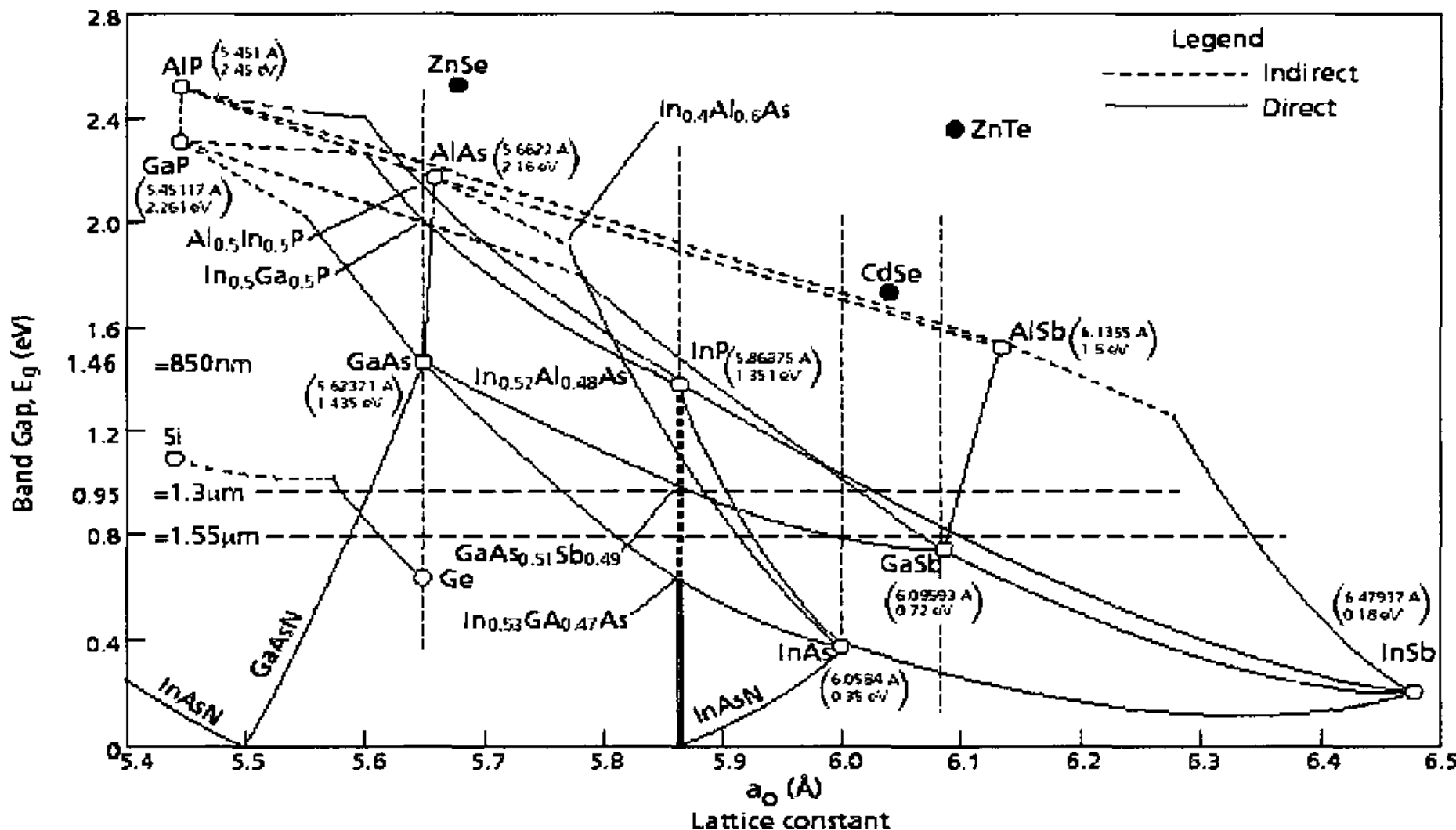
Bandgap engineering

How can we change the heterostructure band structure:

- selecting a material (eg., GaAs / AlAs)
- controlling the composition
- controlling the stress



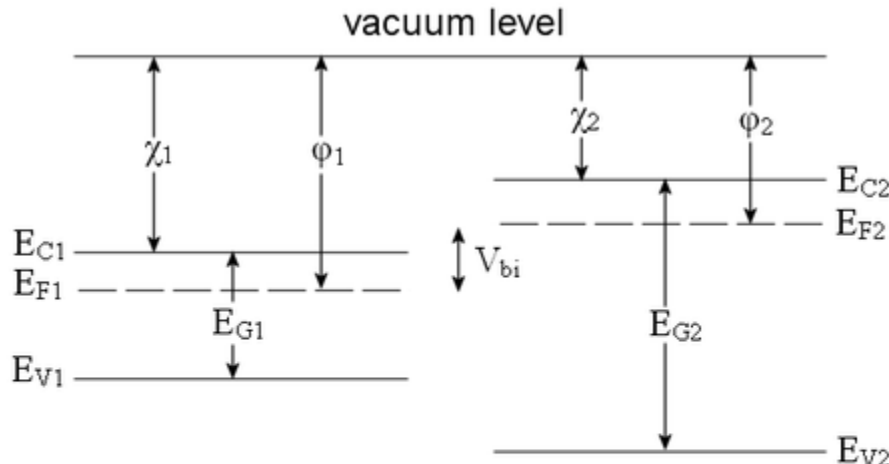
Heterostruktury półprzewodnikowe



Investigation of high antimony-content gallium arsenic nitride-gallium arsenic antimonide heterostructures for long wavelength application

Bandgap engineering

Valence band offset (Anderson's rule)



ϕ = work function

χ = electron affinity (powinowactwo)

E_G = band gap

E_C = conduction band

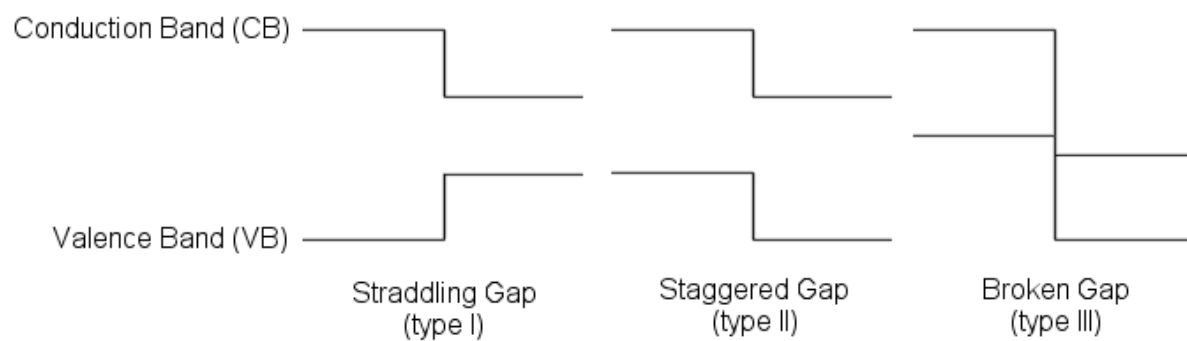
E_V = valence band

$$\Delta E_C = \chi_1 - \chi_2 = \Delta \chi$$

$$\Delta E_G = E_{G2} - E_{G1}$$

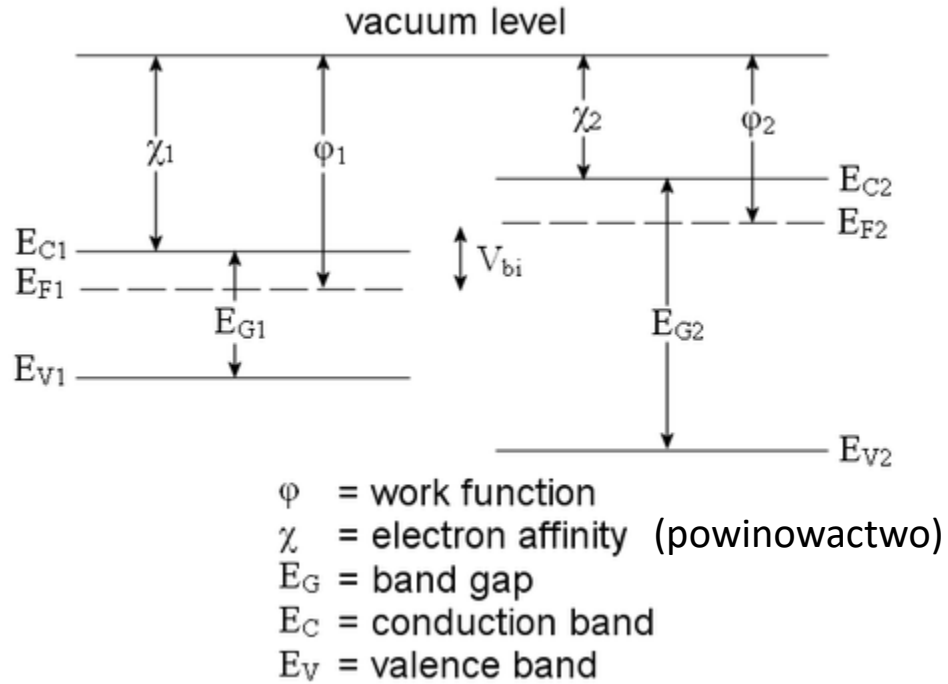
$$\text{Valence band offset: } \Delta E_V = \Delta E_G - \Delta \chi$$

$$\Delta E_G = \Delta E_C + \Delta E_V$$



Bandgap engineering

Valence band offset (Anderson's rule)

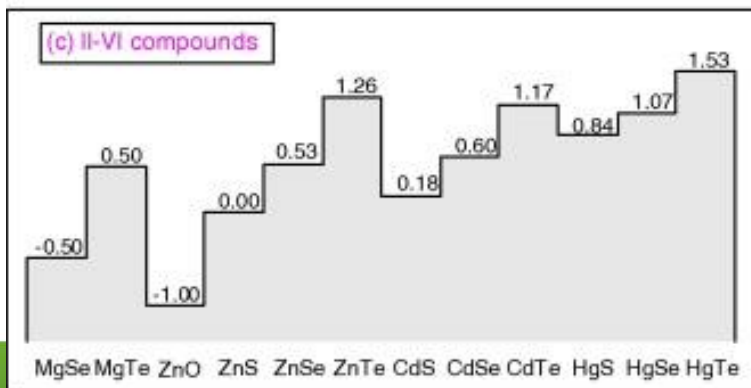
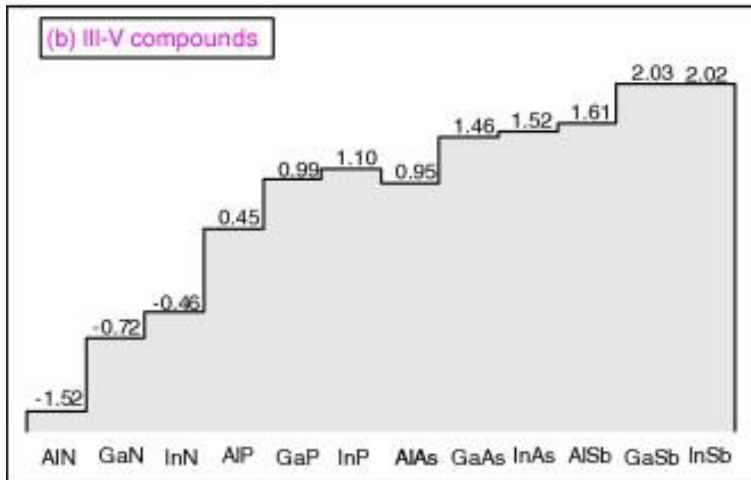
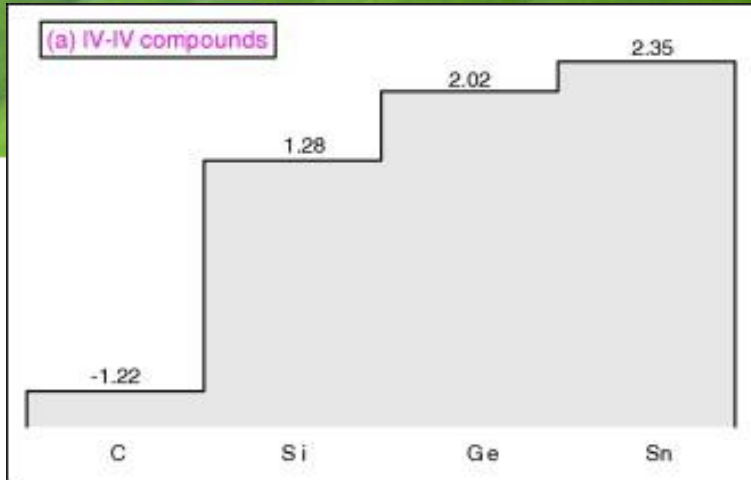


$$\Delta E_C = \chi_1 - \chi_2 = \Delta \chi$$

$$\Delta E_G = E_{G2} - E_{G1}$$

Valence band offset: $\Delta E_V = \Delta E_G - \Delta \chi$

$$\Delta E_G = \Delta E_C + \Delta E_V$$



Bandgap engineering

Valence band offset

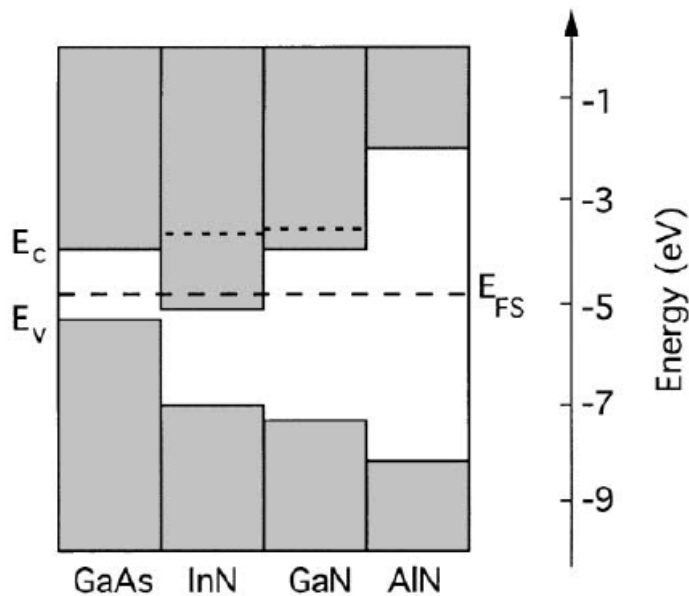


Fig. 4. Band offsets for group III-Nitrides. The dashed lines represent the Fermi energy for the maximum achievable free electron concentration in GaN and InN.

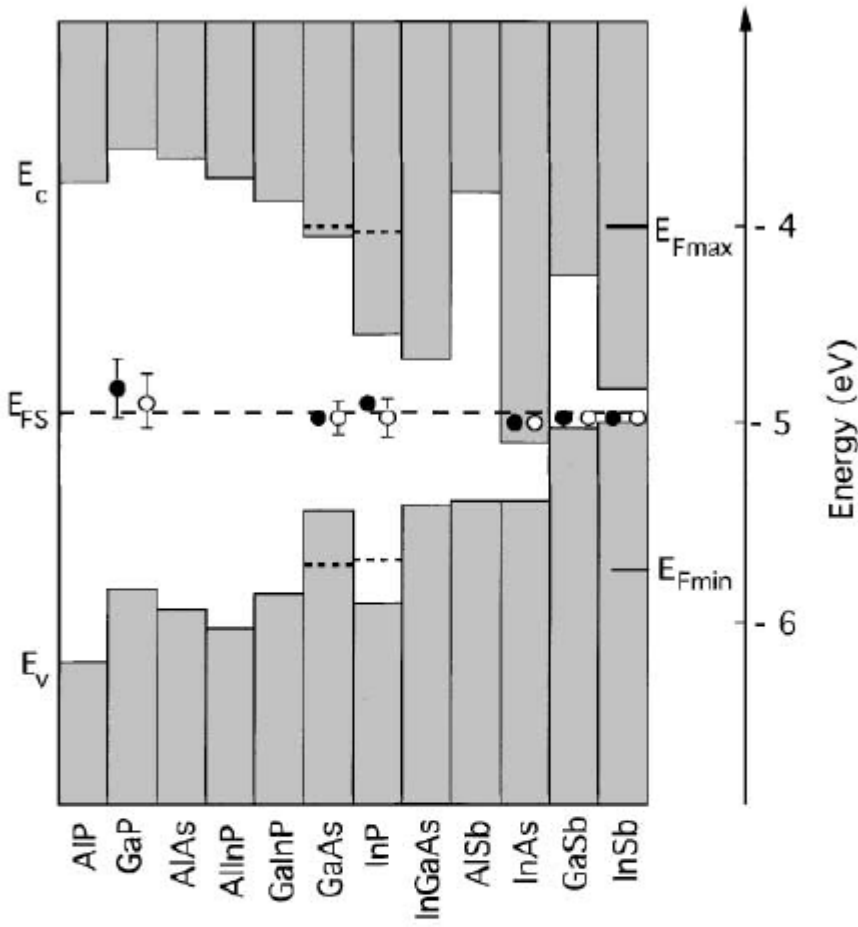


Fig. 1. Band offsets and the Fermi level stabilization energy (E_{FS}) in III-V compounds. The energy is measured relative to the vacuum level. The filled circles represent stabilized Fermi energies in heavily damaged materials, exposed to high energy radiation. The open circles correspond to the location of the Fermi energy on pinned semiconductor surfaces and at metal/semiconductor interfaces. The dashed lines show the location of the Fermi energy for a maximum equilibrium n- and p-type doping in GaAs and InP.

Bandgap engineering

How can we change the heterostructure band structure:

- selecting a material (eg., GaAs / AlAs)
- controlling the composition
- controlling the stress

Vegard's law:

the **empirical heuristic** that the lattice parameter of a solid solution of two constituents is approximately equal to a rule of mixtures of the two constituents' (A and B) lattice parameters at the same temperature:

$$a = a_A(1 - x) + a_Bx$$

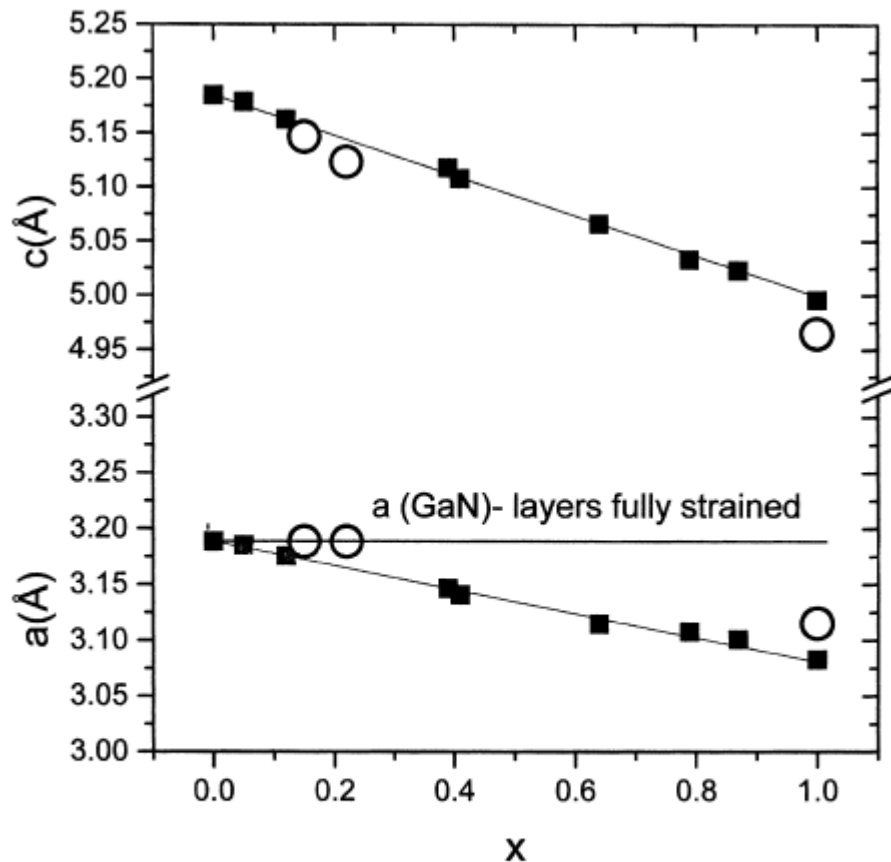


Fig. 5. Lattice parameters of 0.15–0.20 μm $\text{Al}_x\text{Ga}_{1-x}\text{N}$ layers. Lines—Vegard's law between values for the AlN and GaN single crystals, Solid squares— layers on SiC, Open circles— layers on bulk GaN.

Bandgap engineering

How can we change the heterostructure band structure:

- selecting a material (eg., GaAs / AlAs)
- controlling the composition
- controlling the stress

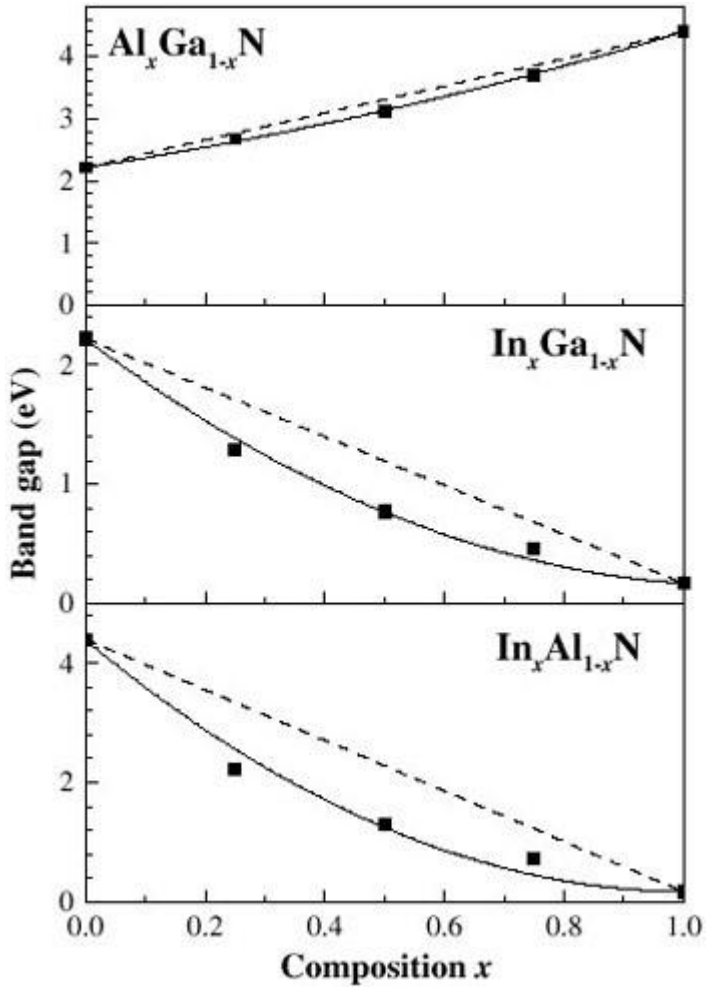
Vegard's law:

Relationship to band gaps of „binary compound”:

$$E = E_A(1 - x) + E_Bx - bx(1 - x)$$

b – so-called „bowing” (curvature) of the energy gap

Tutaj 08.10.2015



A wave packet

$$\psi(x,0) = A \exp\left(-\frac{x^2}{2a^2} + ik_0x\right)$$

$$\begin{aligned} 1 &= \int_{-\infty}^{\infty} dx |\psi(x,0)|^2 = |A|^2 \int_{-\infty}^{\infty} dx \exp\left(-\frac{x^2}{a^2}\right) \\ &= |A|^2 a \sqrt{\pi} \quad \Rightarrow \quad A = \left(\frac{1}{a^2 \pi}\right)^{1/4}, \end{aligned}$$

$$\psi(x,0) = \sqrt{\frac{1}{a\sqrt{\pi}}} \exp\left(-\frac{x^2}{2a} + ik_0x\right)$$

$$\rho(x,0) = \frac{1}{a\sqrt{\pi}} \exp\left(-\frac{x^2}{a^2}\right)$$

$$\Delta x = a$$

A wave packet

$$i\hbar \frac{\partial}{\partial t} \psi(\vec{r}, t) = -\frac{\hbar^2}{2m} \nabla^2 \psi(\vec{r}, t) + V(\vec{r}, t) \psi(\vec{r}, t)$$

$$\psi(x, t) = \int_{-\infty}^{\infty} dk C(k) e^{ikx - i\omega t} \quad \hbar\omega - \frac{\hbar^2 k^2}{2m} = 0$$

Note that

$$\psi(x, 0) = \int_{-\infty}^{\infty} dk C(k) e^{ikx} \quad \text{is a fourrier transform of } C(k) = \frac{1}{2\pi} \int_{-\infty}^{\infty} dx \psi(x, 0) e^{-ikx}$$

Gaussian packet:

$$C(k) = \frac{1}{2\pi} \left(\frac{1}{a^2\pi} \right)^{1/4} \int_{-\infty}^{\infty} dx \exp \left[-\frac{x^2}{2a^2} + i(k_0 - k)x \right]$$

$$\int_{-\infty}^{\infty} dy e^{-\alpha y^2 + \beta y} = \sqrt{\frac{\pi}{\alpha}} \exp \left(\frac{\beta^2}{4\alpha} \right)$$

A wave packet

$$C(k) = \left(\frac{a^2}{4\pi^3} \right)^{1/4} \exp \left[- \frac{1}{2} a^2 (k_0 - k)^2 \right]$$

$$\left(\frac{a^2}{4\pi^3} \right)^{1/4} = \frac{aA}{\sqrt{2\pi}}.$$

$$|C(k)|^2 = \left(\frac{a^2}{4\pi^3} \right)^{1/2} \exp \left[- a^2 (k_0 - k)^2 \right]$$

Gaussian packet:

$$C(k) = \frac{1}{2\pi} \left(\frac{1}{a^2\pi} \right)^{1/4} \int_{-\infty}^{\infty} dx \exp \left[- \frac{x^2}{2a^2} + i(k_0 - k)x \right]$$

$$\int_{-\infty}^{\infty} dy e^{-\alpha y^2 + \beta y} = \sqrt{\frac{\pi}{\alpha}} \exp \left(\frac{\beta^2}{4\alpha} \right)$$

A wave packet

$$\psi(x,t) = \frac{aA}{\sqrt{2\pi}} \int_{-\infty}^{\infty} dk \exp \left[-\frac{a^2}{2} (k - k_0)^2 + ikx - \frac{i\hbar k^2}{2m} t \right]$$

Derivation:

$$\begin{aligned} w &= -\frac{a^2}{2} (k^2 - 2kk_0 + k_0^2) + ikx - \frac{i\hbar t}{2m} k^2 \\ &= -k^2 \left(\frac{a^2}{2} + \frac{i\hbar t}{2m} \right) + k (a^2 k_0 + ix) - \frac{k_0^2 a^2}{2} \\ &= -\alpha k^2 + \beta k - \frac{1}{2} k_0^2 a^2, \end{aligned}$$

$$\psi(x,t) = \frac{aA}{\sqrt{2\pi}} \exp \left(-\frac{1}{2} k_0^2 a^2 \right) \int_{-\infty}^{\infty} dk e^{-\alpha k^2 + \beta k}$$

$$\int_{-\infty}^{\infty} dy e^{-\alpha y^2 + \beta y} = \sqrt{\frac{\pi}{\alpha}} \exp \left(\frac{\beta^2}{4\alpha} \right)$$

A wave packet

$$\begin{aligned}\psi(x, t) &= \frac{aA}{\sqrt{2\pi}} \exp\left(-\frac{1}{2}k_0^2 a^2\right) \sqrt{\frac{\pi}{\alpha}} \exp\left(\frac{\beta^2}{4\alpha}\right) \\ &= \frac{aA}{\sqrt{2\pi}} \left(\frac{\pi}{\frac{a^2}{2} + \frac{i\hbar}{2m}}\right)^{1/2} \exp\left[-\frac{1}{2}k_0^2 a^2 + \frac{(a^2 k_0 + ix)^2}{4\left(\frac{a^2}{2} + \frac{i\hbar}{2m}\right)}\right] \\ &= \frac{A}{\sqrt{1+i\sigma t}} \exp\left[-\frac{1}{2}k_0^2 a^2 + \frac{(a^2 k_0 + ix)^2}{2a^2(1+i\sigma t)}\right], \quad \sigma = \frac{\hbar}{ma^2}\end{aligned}$$

$$\int_{-\infty}^{\infty} dy e^{-\alpha y^2 + \beta y} = \sqrt{\frac{\pi}{\alpha}} \exp\left(\frac{\beta^2}{4\alpha}\right)$$

A wave packet

Ordering expression:

$$w' = -\frac{1}{2}k_0^2a^2 + \frac{k_0^2a^4 + 2ik_0xa^2 - x^2}{2a^2(1 + i\sigma t)}$$

$$= \frac{-x^2 + 2ik_0xa^2 - i\sigma tk_0^2a^4}{2a^2(1 + i\sigma t)}.$$

$$w' = \frac{-x^2 + ik_0x(2a^2 + 2a^2i\sigma t) - ik_0x \cdot 2a^2i\sigma t - i\sigma tk_0^2a^4}{2a^2(1 + i\sigma t)}$$

$$= ik_0x + \frac{-x^2 + 2k_0xa^2\sigma t - i\sigma tk_0^2a^4}{2a^2(1 + i\sigma t)}$$

$$w' = ik_0x + \frac{-x^2 + 2k_0xa^2\sigma t - k_0^2a^4\sigma^2t^2 + k_0^2a^4\sigma^2t^2 - i\sigma tk_0^2a^4}{2a^2(1 + i\sigma t)}$$

$$= ik_0x + \frac{-(x - k_0a^2\sigma t)^2 - i\sigma tk_0^2a^4 - k_0^2a^4(i\sigma t)^2}{2a^2(1 + i\sigma t)}$$

$$= ik_0x - \frac{(x - k_0a^2\sigma t)^2}{2a^2(1 + i\sigma t)} - \frac{1}{2}i\sigma tk_0^2a^2.$$

A wave packet

Ordering expression:

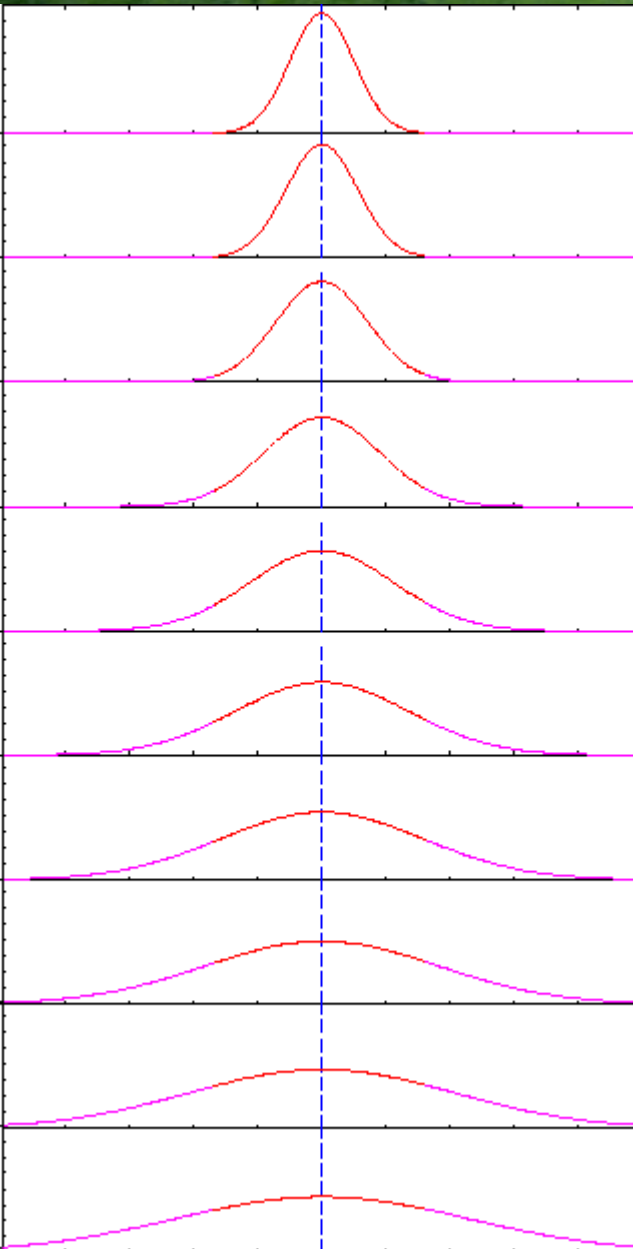
$$k_0 a^2 \sigma = k_0 a^2 \frac{\hbar}{ma^2} = \frac{\hbar k_0}{m} = v_0,$$

$$\frac{1}{2} \sigma k_0^2 a^2 = \frac{1}{2} v_0 k_0 = \frac{\hbar k_0^2}{2m} = \omega_0.$$

$$w' = ik_0x - i\omega_0t - \frac{(x - v_0t)^2}{2a^2(1 + i\sigma t)}$$

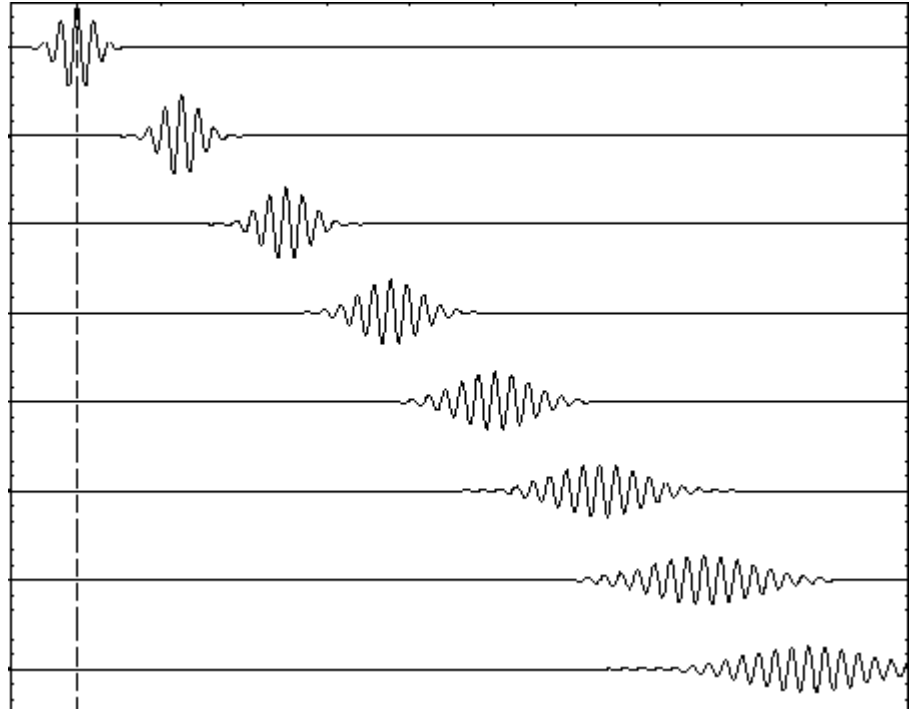
$$\psi(x, t) = \frac{A}{\sqrt{1 + i\sigma t}} e^{ik_0x - i\omega_0t} \exp \left[-\frac{(x - v_0t)^2}{2a^2(1 + i\sigma t)} \right]$$

Pakiet falowy



$$\psi(x, 0) = A \exp\left(-\frac{x^2}{2a^2} + ik_0x\right) \quad \sigma = \frac{\hbar}{ma^2}$$

$$\boxed{\psi(x, t) = \frac{A}{\sqrt{1+i\sigma t}} e^{ik_0x-i\omega_0t} \exp\left[-\frac{(x-v_0t)^2}{2a^2(1+i\sigma t)}\right]}$$



A wave packet

$$\psi(x, 0) = A \exp\left(-\frac{x^2}{2a^2} + ik_0x\right) \quad \sigma = \frac{\hbar}{ma^2}$$

$$\boxed{\psi(x, t) = \frac{A}{\sqrt{1 + i\sigma t}} e^{ik_0x - i\omega_0t} \exp\left[-\frac{(x - v_0t)^2}{2a^2(1 + i\sigma t)}\right]}$$

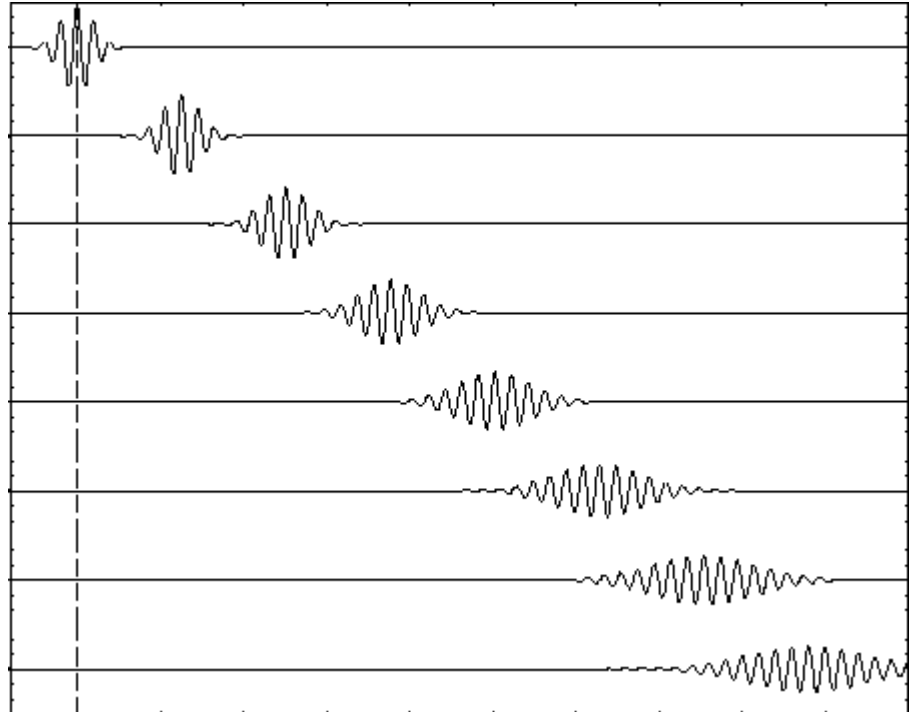
$$\Delta x \Delta p \geq \frac{\hbar}{2}$$

$$m_e = 9.11 \cdot 10^{-31} \text{ kg}$$

$$h = 6.626 \cdot 10^{-34} \text{ Js} = 4.136 \cdot 10^{-15} \text{ eV s}$$

$$\hbar = 1.055 \cdot 10^{-34} \text{ Js} = 6.582 \cdot 10^{-16} \text{ eV s}$$

$$e = -1.602 \cdot 10^{-19} \text{ C}$$



A wave packet

$$|\psi(x)|^2 = |\textcolor{brown}{a}|^2 \exp\left[-\frac{1}{2}\left(\frac{x}{\sigma_x}\right)^2\right]$$

$$\textcolor{brown}{a} = (2\pi\sigma_x^2)^{-1/4}$$

$$\begin{aligned}\sigma^2 &= \langle (x - \langle x \rangle)^2 \rangle \\ &= \langle \textcolor{brown}{x}^2 - 2\textcolor{brown}{x}\langle x \rangle + \langle x \rangle^2 \rangle\end{aligned}$$

$$\sigma^2 = \langle \textcolor{brown}{x}^2 \rangle - 2\langle x \rangle \langle x \rangle + \langle x \rangle^2$$

$$= \langle \textcolor{brown}{x}^2 \rangle - \langle x \rangle^2$$

$$\sigma^2 = \int x^2 |\psi(x)|^2 dx = \sigma_x^2$$

$$A(k) = (8\pi\sigma_x^2)^{1/4} \exp\left[-\sigma_x^2 k^2\right]$$

$$|A(k)|^2 = (8\pi\sigma_x^2)^{1/2} \exp\left[-2\sigma_x^2 k^2\right]$$

$$\frac{1}{2\sigma_k^2} \equiv 2\sigma_x^2 \quad |\sigma_x \sigma_k| = \frac{1}{2} \quad |\sigma_x| |\sigma_{\textcolor{brown}{k}}| \geq |\sigma_x \sigma_k| \quad |\sigma_x| |\sigma_k| \geq \frac{1}{2}$$

A wave packet

Mass particle (electron) and massless (photon)

$$\psi(x, t) = \int_{-\infty}^{\infty} A(k) e^{i(kx - \omega(k)t)} dk$$

A(k) = $e^{-\alpha(k - k_0)^2}$



$$\omega(k) = \omega(k_0) + \frac{d\omega}{dk} \Big|_{k_0} (k - k_0) + \frac{1}{2} \frac{d^2\omega}{dk^2} \Big|_{k_0} (k - k_0)^2$$

foton $\omega = kc$

elektron $\omega = \frac{\hbar k^2}{2m}$

$$\omega(k) = \omega_0 + v_g(k - k_0) + \beta(k - k_0)^2$$

$$\psi(x, t) = \sqrt{\frac{\pi}{\alpha + i\beta t}} e^{i(k_0 x - \omega_0 t)} e^{\frac{-(x - v_g t)^2}{4(\alpha + i\beta t)}}$$

$$|\psi(x, t)|^2 = \frac{\pi}{\sqrt{\alpha^2 + \beta^2 t^2}} e^{\frac{-\alpha(x - v_g t)^2}{2(\alpha^2 + \beta^2 t^2)}}.$$